International Journal of Bifurcation and Chaos, Vol. 9, No. 1 (1999) 119–153

PLANE MAPS WITH DENOMINATOR. I. SOME GENERIC PROPERTIES

GIAN-ITALO BISCHI*
Istituto di Scienze Economiche, University of Urbino, Italy

LAURA GARDINI†
Istituto di Matematica "Levi", University of Parma, Italy
and Istituto di Scienze Economiche, University of Urbino, Italy

CHRISTIAN MIRA‡
Groupe d'Etudes des Systèmes Non Linéaires et Applications,
INSA Complexe Scientifique de Rangueil, 31077 Toulose Cedex, France

Received April 16, 1998; Revised July 8, 1998

This paper is devoted to the study of some global dynamical properties and bifurcations of two-dimensional maps related to the presence, in the map or in one of its inverses, of a vanishing denominator. The new concepts of *focal points* and of *prefocal curves* are introduced in order to characterize some new kinds of contact bifurcations specific to maps with denominator. The occurrence of such bifurcations gives rise to new dynamic phenomena, and new structures of basin boundaries and invariant sets, whose presence can only be observed if a map (or some of its inverses) has a vanishing denominator.

1. Introduction

Maps of $\Re^2$, defined by $x' = F(x, y)$, $y' = G(x, y)$, with at least one of the components F or G given by a fractional rational function, are often met in applications (see e.g. [Marimon & Sunder, 1994; Billings & Curry, 1996, 1997; Bischi & Naimzada, 1995, 1997; Barucci *et al.*, 1997]). If a denominator can vanish, then the map is not defined in the whole plane and some particular behaviors can be related to this fact. In particular, if one of the components of the map (or of its inverses) assumes the form $0/0$ in a point of $\Re^2$, then some peculiar dynamic properties of the map can be evidenced, related to the presence of such points.

In this paper the new concepts of *focal point* and *prefocal curve* are introduced, in order to characterize the particular geometric and dynamic properties, together with some new kinds of bifurcations, peculiar of maps with denominator. Roughly speaking, a *prefocal curve* is a set of points for which at least one inverse exists which maps (or "focalizes") the whole set into a single point, called *focal point*. These concepts have been introduced for the first time during the ECIT (European Conference on Iteration Theory) held in Urbino in September 1996, by the authors of this paper (see [Mira, 1996; Gardini & Bischi, 1996].[1] However, some observations on the role of the vanishing denominator and of the points in which a map (or its inverses)

*E-mail: bischi@econ.uniurb.it
†E-mail: gardini@econ.uniurb.it
‡E-mail: mira@insa-tlse.fr

[1]In [Mira, 1996], instead of "focal point" the term "focalization point" is used, whose definition is related to the structure of the phase curves of the map T. In [Gardini & Bischi, 1996] the term "set of focal values" is used instead of "prefocal curve".

assumes the form 0/0 were already present in a paper by Mira [1981] (see also [Mira *et al.*, 1996, p. 25]).

In this paper we study some generic properties of two-dimensional fractional rational maps that are not defined in the whole plane, due to the presence, in at least one component of the map, of a denominator that can vanish. The definitions of focal points and prefocal curves are given, and their effects on the geometrical properties of a rational map are described. Such effects are studied by considering the image, by a rational map, of a curve of the plane crossing through the set of points in which a denominator vanishes (called *set of nondefinition*) and, in particular, the images of curves crossing through the particular point of this set called *focal point*. In the generic case a one-to-one correspondence is obtained between the slopes of the arcs through a focal point and the points in which their images cross the corresponding prefocal curve. This implies that the preimages of any curve crossing the prefocal curve in two points are given by loops with a kind of double point in the focal point. This property may be very important in order to characterize some particular structures of the basins boundaries, as shown in some previous papers [Mira, 1996; Bischi & Gardini, 1996, 1997] and in some examples given in the present one.

The geometric effects of focal points and prefocal curves, on the images and preimages of a generic curve of the plane, become particularly important for the properties of the iterated map (i.e. from a dynamical point of view) if images and preimages of phase curves are considered. Phase curves are invariant curves for the map, such as the boundaries of basins, stable sets and unstable sets of cycles.

New kinds of bifurcations, peculiar of maps with denominator, are explained by contacts between basin boundaries and prefocal curves. These bifurcations cause the creation of particular structures of the basin boundaries, denoted as *lobes* and *crescents*, giving rise to fans of such figures centered at the focal points, and belonging to the stable sets that constitute the boundaries of the basins. Such particular structures have been recently observed in [Bischi & Gardini, 1996, 1997; Mira, 1996; Billings & Curry, 1996; Billings *et al.*, 1997; Brock & Hommes, 1997].

A contact between the unstable set of a saddle fixed point (or a saddle cycle) and the set of nondefinition, locus of points in which a denominator vanishes, generally causes the sudden creation of unbounded branches of the unstable set, thus giving a new mechanism for the occurrence of homoclinic bifurcations, specific to maps with a vanishing denominator.

The bifurcations due to tangential contacts between arcs of phase curves (like those that form the basin boundaries, or the unstable sets of saddles) and a prefocal curve or a set of nondefinition, are denoted as *bifurcations of first class*. Other important bifurcations (for example due to the merging of focal points, or to the merging of focal points and fixed points, or to contacts between prefocal curves and critical curves) shall be denoted as *bifurcations of second class*, and are not considered in the present paper (these will be studied in a second paper, in preparation). In the present paper the situations related to bifurcations of second class are considered nongeneric.

The theory of focal points and prefocal curves is also useful to understand some properties of maps without denominator, having at least one inverse map with vanishing denominator. Such maps may have the property that among the points at which the Jacobian vanishes there exists a curve $\mathcal{C}$ which is mapped into one single point P. Such property, that was already observed in the study of some polynomial maps [Cathala & Barugola, 1996; Mira *et al.*, 1996, p. 197, p. 228] is related to the fact that the curve $\mathcal{C}$ is a prefocal curve of at least one inverse, the point P being the related focal point.

Another noticeable property of these maps is that a curve $\mathcal{S}$ at which the denominator of some inverse vanishes may separate regions of the phase plane characterized by a different number of preimages, even if it is not a critical curve of rank-1 (a critical curve of rank-1 is defined as a set of points having at least two merging rank-1 preimages, see [Gumowski & Mira, 1980; Mira *et al.*, 1996]. We show that at least one inverse is not defined on these noncritical boundary curves, due to the vanishing of some denominator. The role of such a curve is the analogue, in a two-dimensional map, of an horizontal asymptote in a one-dimensional map, that can separate the range into intervals with different numbers of rank-1 preimages.

The existence of focal points of an inverse map can also cause the creation of particular attracting sets because, as we shall see in one of the examples shown in Sec. 3, a focal point of the inverse map may behave like a "knot" where infinitely many

invariant curves of an attracting set shrink into a single point.

The plan of the paper is the following. In Sec. 2 definitions and geometric properties, together with the general description of some contact bifurcations of the first class, are illustrated by several examples. In Sec. 3 some polynomial maps are considered whose inverses have focal points. Some of these maps have already been studied in the literature, but here they are reconsidered at the light of the new methods and concepts on rational maps proposed in the present paper. In Sec. 4 a general formulation of the problems and the concepts exposed in this paper is given by using an implicit form for maps of the plane, from which at least one explicit map with denominator is obtained.

2. Rational Maps with Focal Points and Prefocal Curves

2.1. *Definitions and basic properties*

In this section we give some definitions and some generic properties related to maps $(x, y) \to (x', y') = T(x, y)$ of the form

$$T : \begin{cases} x' = F(x, y) \\ y' = G(x, y) \end{cases} \tag{1}$$

where x and y are real variables and at least one of the components has the form of a fractional rational function, i.e.

$$F(x, y) = \frac{N_1(x, y)}{D_1(x, y)}$$

and/or
$$G(x, y) = \frac{N_2(x, y)}{D_2(x, y)}\,. \tag{2}$$

Some concepts and properties given in this section will also be reconsidered, in a more general framework, in Sec. 4.

In order to simplify the exposition, in the following we assume that only one of the two functions F and G has a denominator that can vanish, for example $G(x, y) = N(x, y)/D(x, y)$, so that the map (1) becomes

$$T : \begin{cases} x' = F(x, y) \\ y' = \dfrac{N(x, y)}{D(x, y)} \end{cases} \tag{3}$$

where, without loss of generality, we assume that the functions $F(x, y)$, $N(x, y)$ and $D(x, y)$ are defined in the whole plane $\Re^2$. For the maps considered in this paper the set of nondefinition δ_s coincides with the locus of points in which at least one denominator vanishes. For the map (3) it is given by

$$\delta_s = \{(x, y) \in \Re^2 | D(x, y) = 0\}\,. \tag{4}$$

In the following we assume that δ_s is a smooth curve of the plane. The two-dimensional recurrence obtained by the iteration of T is well defined provided that the initial condition belongs to the set E given by

$$E = \Re^2 \Big\backslash \bigcup_{k=0}^{\infty} T^{-k}(\delta_s)\,. \tag{5}$$

In fact, the points of the singular set, as well as all their preimages of any rank, which constitute a set of zero lebergue measure, must be excluded from the set of initial conditions that generate well defined sequences by the iteration of the map T, so that $T : E \to E$.

In order to define the concepts of *focal point* and *prefocal curve* we consider a smooth simple arc γ transverse to δ_s and we study how it is transformed by the application of the map T, i.e. what is the shape of its rank-1 image $T(\gamma)$. On taking the image $T(\gamma)$, we assume that the arc γ is deprived of the point in which it intersects δ_s. Let (x_0, y_0) be this point and assume that in a neighborhood of (x_0, y_0) γ is represented by the parametric equations

$$\gamma(\tau) : \begin{cases} x(\tau) = x_0 + \xi_1\tau + \xi_2\tau^2 + \cdots \\ y(\tau) = y_0 + \eta_1\tau + \eta_2\tau^2 + \cdots \end{cases} \qquad \tau \neq 0\,. \tag{6}$$

The portion of γ in such a neighborhood can be seen as the union of two disjoint pieces, say $\gamma = \gamma_- \cup \gamma_+$, where γ_- and γ_+ denote the portions of γ located on opposite sides with respect to the singular curve δ_s, obtained from (6) with $\tau < 0$ and $\tau > 0$ respectively. The closure $\overline{\gamma(\tau)}$ is such that $\overline{\gamma_-(0)} = \overline{\gamma_+(0)} = (x_0, y_0)$ (Fig. 1). As $(x_0, y_0) \in \delta_s$ we have, according to the definition (4) of δ_s, $D(x_0, y_0) = 0$, but in general $N(x_0, y_0) \neq 0$. Hence

$$\lim_{\tau \to 0} T(\gamma(\tau)) = (F(x_0, y_0), \infty) \tag{7}$$

where ∞ means either $+\infty$ or $-\infty$. This means that the image $T(\gamma)$ is made up of two disjoint unbounded arcs asymptotic to the line of equation

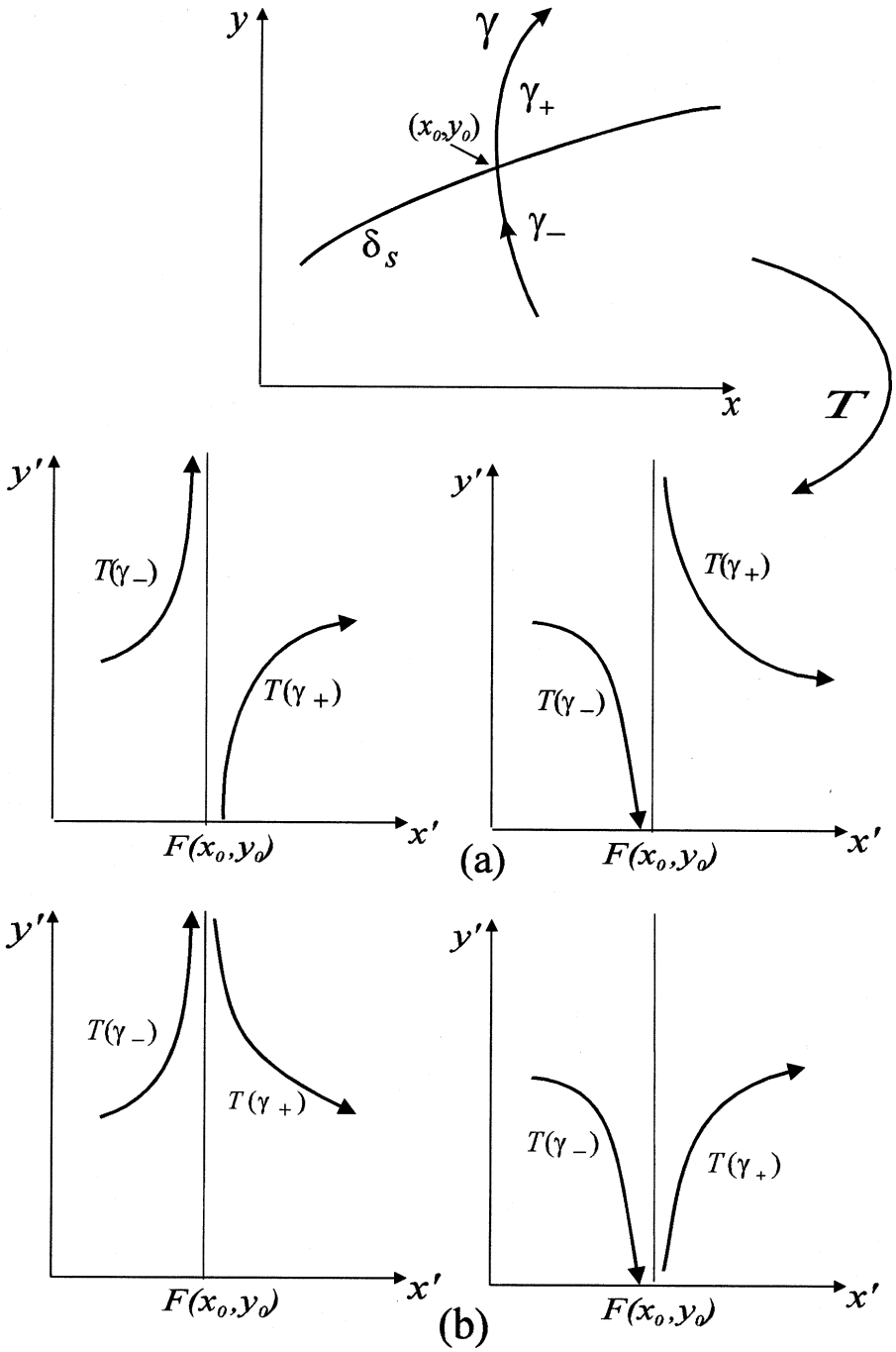

Figure 1.

$x = F(x_0, y_0)$ (see Fig. 1). If the denominator $D(x, y)$ changes sign as the point (x, y) crosses δ_s, moving along the arc γ, then the two unbounded branches of $T(\gamma)$ are asymptotic to the line $x = F(x_0, y_0)$ as in Fig. 1(a), otherwise one of the situations shown in Fig. 1(b) is obtained.

A different situation may occur if the point $(x_0, y_0) \in \delta_s$ is such that not only the denominator but also the numerator of (3) vanishes in it, i.e. $D(x_0, y_0) = N(x_0, y_0) = 0$. In this case, in the limit (7) the second component assumes the form of zero over zero. This implies that, in contrast with (7), the limit may give a finite value, so that the image $T(\gamma)$ is a bounded arc crossing the line $x = F(x_0, y_0)$ in the point $(F(x_0, y_0), y)$, where

$$y = \lim_{\tau \to 0} G(x(\tau), y(\tau)) . \tag{8}$$

Of course, the value y of the limit (8) depends on the arc γ. Furthermore it may have a finite value along some arcs and be infinite along other ones. This leads us to the following definition:

Definition 1. Consider the map (1). A point $Q = (x_0, y_0)$ is a focal point if at least one component of the map T takes the form $0/0$ in Q and there exist smooth simple arcs $\gamma(\tau)$, with $\gamma(0) = Q$, such that $\lim_{\tau \to 0} T(\gamma(\tau))$ is finite. The set of all such finite values, obtained by taking different arcs $\gamma(\tau)$ through Q, is the prefocal set δ_Q.

The reasons for the choice of the terms focal and prefocal will become clear when the behavior of the inverse (or the inverses) of T will be analyzed. It is plain that in the particular case analyzed in this section, in which the map T has the form (3), the prefocal set δ_Q belongs to the line of equation $x = F(Q)$ (Fig. 2).

In this paper we shall only consider simple focal points, defined as focal points which are simple roots of the algebraic system

$$\begin{cases} N(x, y) = 0 \\ D(x, y) = 0 \end{cases} \tag{9}$$

i.e. a focal point $Q = (x_0, y_0)$ is simple if

$$\overline{N}_x \overline{D}_y - \overline{N}_y \overline{D}_x \neq 0 \tag{10}$$

where $\overline{N}_x = \partial N / \partial x(x_0, y_0)$ and analogously for the other partial derivatives. Focal points which are not simple can only occur in the cases of bifurcations of

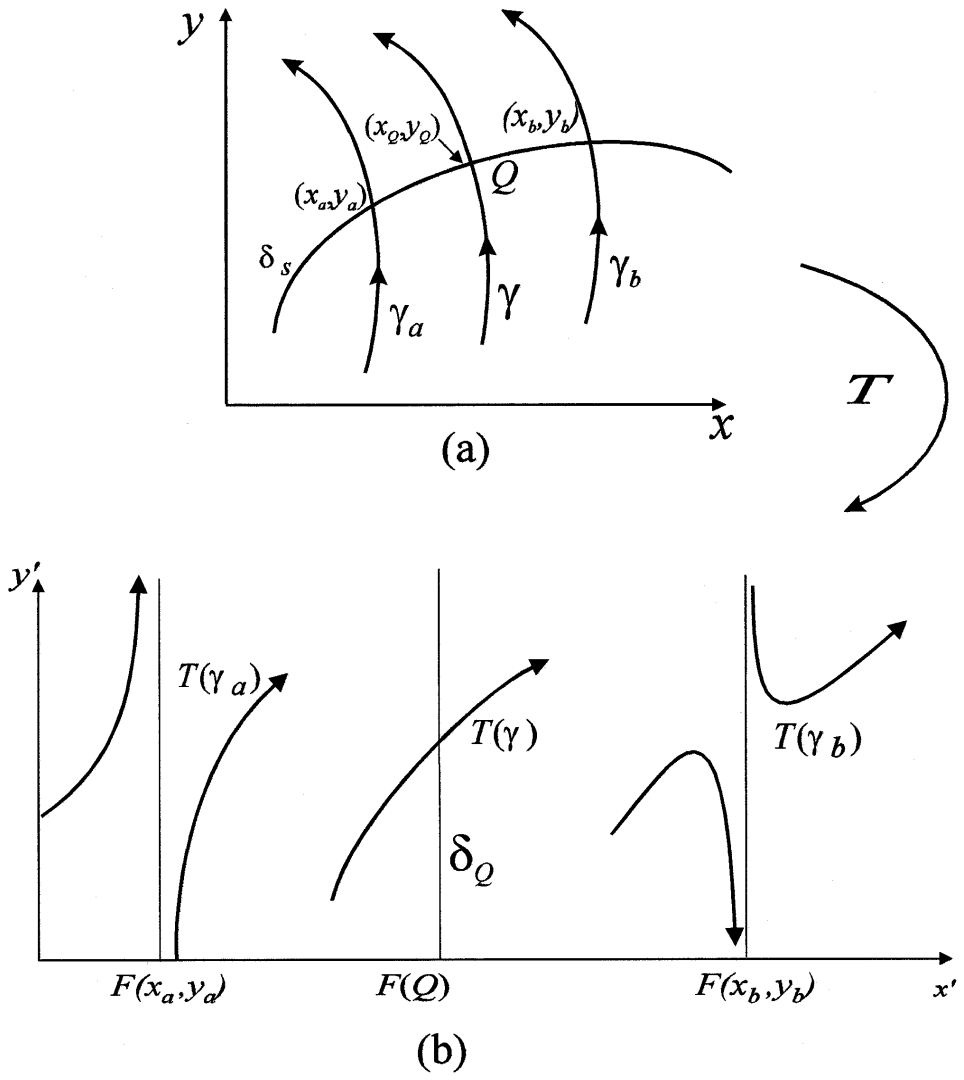

Figure 2.

class two, that, as explained in the introduction, are not considered in the present paper.

We show now that in the case of a simple focal point a one-to-one correspondence between the point $(F(Q), y)$, in which $T(\gamma)$ crosses δ_Q and the slope $m = \eta_1/\xi_1$ of $\overline{\gamma}$ in Q can be obtained. Indeed, let us consider an arc γ, with parametric representation (6), through a focal point $Q = (x_0, y_0)$, and assume that the numerator $N(x, y)$ and the denominator $D(x, y)$ of the second component $G(x, y)$ of T are smooth functions. Since both these functions vanish in Q they can be expressed as

$$N(x, y) = \overline{N_x}(x - x_0) + \overline{N_y}(y - y_0) + O_2$$
$$D(x, y) = \overline{D_x}(x - x_0) + \overline{D_y}(y - y_0) + O_2'$$

where O_2, O_2' represent terms of higher order. If Q is a simple focal point then

$$\lim_{\tau \to 0} G(\gamma(\tau)) = \frac{\overline{N_x}\xi_1 + \overline{N_y}\eta_1}{\overline{D_x}\xi_1 + \overline{D_y}\eta_1}. \qquad (11)$$

Notice that the denominator in (11) is different from zero provided that the slope $m = \eta_1/\xi_1$ of the arc $\overline{\gamma}$ in Q is different from the slope of the curve δ_s in the same point, given by $-\overline{D}_x/\overline{D}_y$. This condition is sufficient to ensure that y, given by (8), is finite. However a finite value of the limit (8) can also be obtained if the arc γ is tangent to δ_s in Q and also the numerator of (11) becomes zero. We do not consider here all such possibilities, since in this paper we are only interested in the generic case in which finite values of y are obtained by (11). Such a generic occurrence allows to define a one-to-one correspondence between the slope $m = \eta_1/\xi_1$ of the arc γ in Q and the point $(F(Q), y)$ in which the image $T(\gamma)$ crosses the prefocal curve δ_Q, as stated by the following Proposition which summarizes the arguments given above:

Proposition 1. *Let T be a fractional rational map in the form (3) and let Q be a simple focal point related to the prefocal curve δ_Q. Then a one-to-one relation between the slope m of an arc γ through Q not tangent to δ_s, and the point $(F(Q), y)$ in which $T(\gamma)$ crosses δ_Q exists, defined by*

$$m \to (F(Q), y(m)),$$

with

$$y(m) = \frac{\overline{N_x} + m\overline{N_y}}{\overline{D_x} + m\overline{D_y}} \qquad (12)$$

and

$$(F(Q), y) \to m(y)$$

with

$$m(y) = \frac{\overline{D_x}y - \overline{N_x}}{\overline{N_y} - \overline{D_y}y}. \qquad (13)$$

From this proposition we deduce that different arcs γ_j, passing through a focal point Q with different slopes m_j, are mapped by T into bounded arcs $T(\gamma_j)$ crossing δ_Q in different points $(F(Q), y(m_j))$, as qualitatively shown in Fig. 3. Interesting properties are obtained if the inverse of T (or the inverses, if T is a noninvertible map) is (are) applied to a curve that crosses a prefocal curve.

Case of an invertible map

Let us first consider the case of an invertible map, and let δ_Q^i be a prefocal curve whose corresponding focal point is Q^i. Being T an invertible map, each point sufficiently close to δ_Q^i has its rank-1

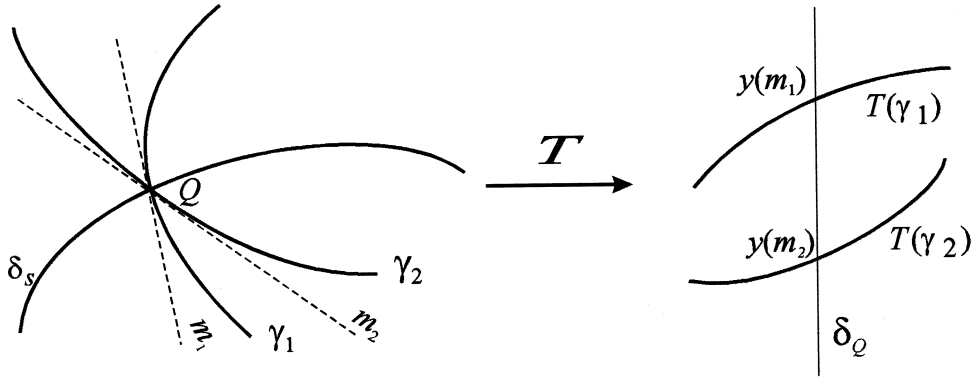

Figure 3.

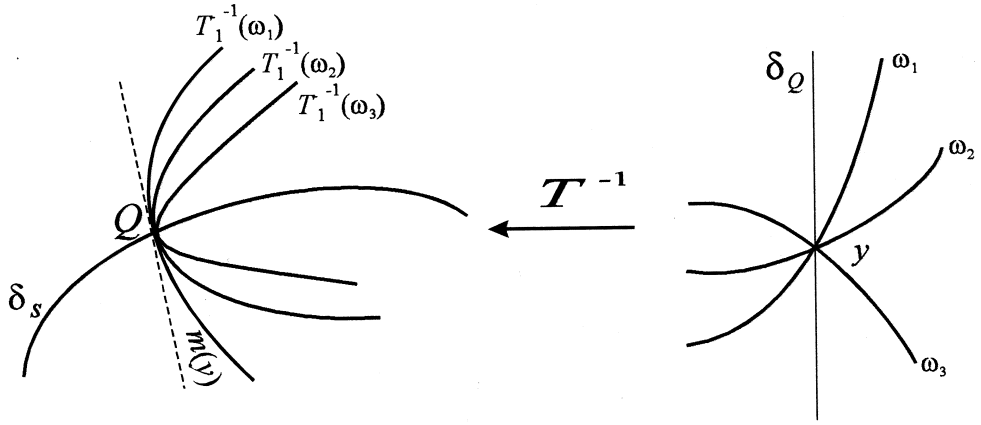

Figure 4.

preimage in a neighborhood of the focal point Q^i. If T^{-1} is continuous along δ_Q^i then all the points of δ_Q^i are mapped by T^{-1} in the focal point Q^i. Roughly speaking,[2] we can say that the prefocal curve δ_Q^i is "focalized" by T^{-1} in the focal point Q^i, or, more concisely, that $T^{-1}\left(\delta_Q^i\right) = Q^i$. We remark that the map T is not defined in Q^i, thus T^{-1} is not to be strictly considered as an inverse of T in the points of δ_Q^i, even if T^{-1} is defined in δ_Q^i.

From (13) we deduce that the preimages of different arcs crossing the prefocal curve δ_Q^i in the same point are given by arcs through Q^i all with the same slope $m_i(y)$ in Q^i. In fact, let us consider different arcs ω_n, crossing δ_Q^i in the same point $(F(Q^i), y)$ with different slopes. These arcs are mapped by the inverse map T^{-1} into different arcs $T^{-1}(\omega_n)$ through Q^i, all with the same tangent of slope $m_i(y)$, according to (13), as qualitatively shown in Fig. 4.

Regarding the geometric behavior of the inverse map T^{-1}, this property of a prefocal curve recalls the properties of a curve in which the Jacobian vanishes (see [Julia, 1929; Gumowski & Mira, 1980; Mira *et al.*, 1996]). Indeed, from the definition of the prefocal curve, it follows that the Jacobian $\det(DT^{-1})$ must necessarily vanish in the points of δ_Q^i. In fact, if the map T^{-1} is defined in δ_Q^i then all the points of the line δ_Q^i are mapped by T^{-1} into the focal point Q^i. This means that T^{-1} is not locally invertible in the points of δ_Q^i, being it a many-to-one map, and this implies that its Jacobian cannot be different from zero in the points of δ_Q^i.

[2]The rigorous treatment of this point of view is given in Sec. 4.

Case of a noninvertible map

In the case of a noninvertible map T, i.e. a map for which $k > 1$ inverses may exist in some regions of the (x, y) plane, several focal points $Q^{i,j}$, $j = 1, \ldots, k$, with $k \geq 2$, are associated with a prefocal curve δ_Q^i, each with its own one-to-one correspondence between slopes and point, as that defined by (12) and (13). We recall that the phase space of a noninvertible map is subdivided into open regions (or zones) Z_k, whose points have k distinct rank-1 preimages, obtained by the application of k distinct inverse maps. In other words, if $(x, y) \in Z_k$ then k distinct points (x_j, y_j) are mapped into (x, y), i.e. $T(x_j, y_j) = (x, y)$ for $j = 1, \ldots, k$, or, equivalently, k distinct inverse maps T_j^{-1} exist such that $T_j^{-1}(x, y) = (x_j, y_j)$, $j = 1, \ldots, k$. A specific feature of noninvertible maps is the existence of the critical set LC (from "Lignes Critique", see [Gumowski & Mira, 1980; Mira *et al.*, 1996]) defined as the locus of points having at least two coincident rank-1 preimages, located on the set of merging preimages denoted by LC_{-1}. Segments of LC are boundaries that separate different regions Z_k, but the converse is not generally true, that is, also in the two-dimensional case, as in the one-dimensional one, boundaries of regions Z_k which are not portions of LC may exist.

We recall that $LC = T(LC_{-1})$, and in the case of a smooth map LC_{-1} belongs to the set of points in which the Jacobian of T vanishes:

$$LC_{-1} \subseteq J_0 = \{(x, y) \in \Re^2 | \det DT = 0\}$$

because in any neighborhood of a point of LC_{-1} there are at least two distinct points mapped by T into the same point, so that the map T is not locally invertible in the points of LC_{-1}.

If we consider a noninvertible map with denominator, in order to avoid bifurcation cases of the second class we shall only consider focal points not belonging to $\overline{LC}_{-1}$. In this case the following proposition holds.

Proposition 2. *If a noninvertible map with denominator has focal points not belonging to* $\overline{LC}_{-1}$ *then for each prefocal curve* δ_Q^i *we have* $LC \cap \delta_Q^i = \emptyset$.

The proof is straightforward by reasoning *ab absurdo*. In fact, if LC intersects a prefocal curve δ_Q^i in a point P, i.e. $P \in \{LC \cap \delta_Q^i\}$, then, according to the definition of LC, at least two preimages of P should merge in a focal point $Q^{i,j} = T_j^{-1}(\delta_Q^i)$ belonging to LC_{-1}, which contradicts the assumption.

In noninvertible maps, in the generic case in which the focal points do not belong to $\overline{LC}_{-1}$, the boundaries that separate regions whose points have a different number of preimages are either formed by points of the critical manifold LC or, as we shall see in Sec. 3, by points in which the denominator of some inverse vanishes. Hence, under the assumptions of Proposition 2, together with the further assumption that all the inverses are continuous along δ_Q^i, we can state the following.

Proposition 3. *If a noninvertible map with denominator has focal points not belonging to* $\overline{LC}_{-1}$ *and all the inverses are continuous along a prefocal curve* δ_Q^i *then* δ_Q^i *belongs to a region* Z_k *in which* k *inverse maps* T_j^{-1}, $j = 1, \ldots, k$, *are defined.*

It is clear that for each δ_Q^i at least one inverse is defined that "focalizes" it into a focal Q^i. However, according to Proposition 3, other inverses (at most k) may exist that "focalize" it into distinct focal points, all associated with the prefocal curve δ_Q^i. These focal points will be denoted as $Q^{i,j} = T_j^{-1}(\delta_Q^i)$, $j = 1, \ldots, n$, with $n \leq k$. For each focal point $Q^{i,j}$ the same results given above can be obtained with T^{-1} replaced by T_j^{-1}, so that for each $Q^{i,j}$ a one-to-one correspondence $m_{i,j}(y)$ in the form (13) is defined. Following arguments similar to those given above, it is easy to see that an arc ω crossing δ_Q^i in the point $(F(Q^{i,j}), y)$ is mapped by each T_j^{-1} into an arc $T_j^{-1}(\omega)$, through the corresponding $Q^{i,j}$, with slope $m_{i,j}(y)$; if different arcs are considered, crossing δ_Q^i in the same point, then these are mapped by each inverse T_i^{-1} into different arcs through $Q^{i,j}$, all with the same tangent, as qualitatively shown in Fig. 5 in the case $n = 2$.

From the discussion above, a different method to find the prefocal curves and the corresponding focal points can be followed, provided that the inverse(s) of the map T is (are) explicitly known. For each inverse T_j^{-1} the locus of points J_0' at which $\det(DT_j^{-1})$ vanishes is found, and the images by T_j^{-1} of the points of J_0' are computed. If J_0' includes a curve δ such that $T_j^{-1}(\delta)$ is a single point

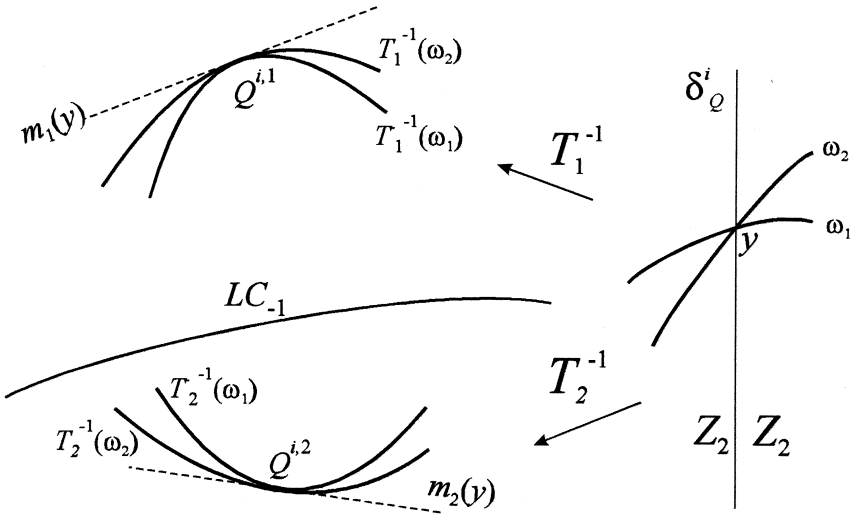

Figure 5.

Q, then that curve is a prefocal curve for the map T and Q is one of the corresponding focal points.

This procedure is at the basis of the definition of prefocal curve given in [Mira, 1996] and also makes clear the choice of the terminology: each curve δ_Q^i is "focalized" into the focal point $Q^{i,j}$ by the action of the inverse map T_j^{-1}.

We now show that from the property $\det(DT_j^{-1}(\delta_Q^i)) = 0$ a different method can be obtained to find the correspondence (13) between the slope of arcs through Q and the points of δ_Q. This method is based on the following classical property of mathematical analysis.

Property. *Let $M : (x, y) \to (x', y')$ be a map of the plane, defined by $(x', y') = M(x, y) = (M_1(x, y), M_2(x, y))$, such that its Jacobian $\det(DM(x, y))$ vanishes along a curve J_0 of the plane, and let A be a point of J_0. Let λ_0 and λ_1 be the eigenvalues of $DM(A)$, given by $\lambda_0 = 0$ and $\lambda_1 = \mathrm{Tr}(DM(A)) = M_{1x}(A) + M_{2y}(A)$, and let $\mathbf{v}_0$ and $\mathbf{v}_1$ be the corresponding eigenvectors. If $\lambda_1 \neq 0$ then all the smooth curve segments passing through A, with slope different from that of $\mathbf{v}_0$, are mapped by M into smooth arcs that have all the same tangent in $B = M(A)$, parallel to the eigenvector v_1. If $DM = [J_{ij}]$, $i, j = 1, 2$, then the eigenvector $\mathbf{v}_1$, corresponding to the eigenvalue $\lambda_1 = J_{11} + J_{22}$, is proportional to one of the two column vectors of DM, so its slope is given by*

$$m_{v_1} = \frac{J_{21}}{J_{11}} \qquad or \qquad m_{v_1} = \frac{J_{22}}{J_{12}}. \tag{14}$$

This property implies that for any curve segment ω that crosses a prefocal curve δ_Q^i in a point $A = (x, y)$, the slope of a preimage $\gamma = T_j^{-1}(\omega)$ in the point $Q^{i,j}$ only depends on the point A, and is independent of the slope of ω in A.

In order to obtain the relation (13) by this different method, let us consider a map in the form (3), and let $Q^{i,j}$ be a focal point, with corresponding prefocal line δ_Q^i of equation $x = F(Q^{i,j})$. Let $T_j^{-1} : (x', y') \to (x, y)$ be the inverse that "focalizes" δ_Q^i into $Q^{i,j}$, i.e. $T_j^{-1}(x', y') = Q^{i,j}$ for each $(x', y') = (F(Q^{i,j}), y) \in \delta_Q^i$, and consider a smooth curve segment $\omega(\tau)$ that crosses δ_Q^i in a point $\omega(0) = A = (F(Q^{i,j}), y)$. Let us consider its preimage $\gamma_j(\tau) = T_j^{-1}(\omega(\tau))$ that crosses δ_s through $Q^{i,j} = T_j^{-1}(\omega(0))$. We know that the Jacobian is such that as $\tau \to 0 \det(T_j^{-1}(\omega(\tau))) \to \det(T_j^{-1}(A)) = 0$. From the theorem on the derivative of the inverse function we have

$$DT_j^{-1}(x', y') = [DT(x(x', y'), y(x', y'))]^{-1}. \tag{15}$$

The Jacobian matrix of (3) is

$$DT(x, y) = \begin{bmatrix} F_x & F_y \\ \dfrac{N_x D - N D_x}{D^2} & \dfrac{N_y D - N D_y}{D^2} \end{bmatrix}$$

hence, from (15), we have

$$DT_j^{-1}(x', y') = \frac{1}{\det(DT)} \begin{bmatrix} \dfrac{N_y D - N D_y}{D^2} & -F_y \\ -\dfrac{N_x D - N D_x}{D^2} & F_x \end{bmatrix}$$

where all the functions in the right hand side are computed in the point $(x(x', y'), y(x', y')) = T_j^{-1}(\omega(\tau)) = \gamma(\tau)$. As $\tau \to 0$ one of the eigenvalues vanishes in the limit, thus the two rows of DT_j^{-1} tend to become proportional. According to (14) the slope of the eigenvector corresponding to the other (nonvanishing) eigenvalue tends to

$$\frac{J_{21}}{J_{11}} = -\frac{N_x D - N D_x}{N_y D - N D_y} = -\frac{N_x - \dfrac{N}{D} D_x}{N_y - \dfrac{N}{D} D_y}.$$

In the limit $\tau \to 0$ this slope becomes

$$\lim_{\tau \to 0} \frac{J_{21}}{J_{11}} = \lim_{\tau \to 0} -\frac{N_x - \dfrac{N}{D} D_x}{N_y - \dfrac{N}{D} D_y} = -\frac{\overline{N_x} - y\overline{D_x}}{\overline{N_y} - y\overline{D_y}} \tag{16}$$

where the overbar means "computed in the focal point". The last equality in (16) follows from the fact that

$$\lim_{\tau \to 0} \frac{N(x(x', y'), y(x', y'))}{D(x(x', y'), y(x', y'))} = \lim_{\tau \to 0} \frac{N(\gamma(\tau))}{D(\gamma(\tau))} = y$$

whichever is the arc $\gamma(\tau) = T_j^{-1}(\omega(\tau))$, preimage of ω passing through Q with slope m_{v_1}, along which the limit is computed (recall that $\omega(\tau)$ is such that $\omega(0) = (F(Q^{i,j}), y)$).

2.2. *Some geometric properties of focal points and prefocal curves*

For a map $(x', y') = T(x, y)$ which is not defined in the whole plane, due to the presence of a vanishing denominator, the existence of the singular set δ_s and of the prefocal curves δ_Q^i, defined in the previous section, may have important effects on the geometrical and dynamical properties of T. On the basis of the results of Sec. 2.1, we now study how a contact between a curve segment γ and the set δ_s causes noticeable qualitative changes in the shape of the image $T(\gamma)$, and how a contact of γ with a prefocal curve δ_Q causes important qualitative changes in the shape of the preimages $T_j^{-1}(\gamma)$.

These contacts may be particularly important when the segments of curves considered are portions of phase curves of the map T, such as *invariant closed curves* as well as *stable or unstable sets* of saddle fixed points or saddle cycles. In these cases the contacts with δ_s or δ_Q can cause the occurrence of new types of global bifurcations that change the structure of the attracting sets or of their basins of attraction, as shown in [Mira, 1996; Bischi & Gardini, 1996, 1997], as well as in the new examples proposed in this paper.

To understand the geometric and dynamical properties of fractional rational maps, and their particular global bifurcations, we assume that δ_s and δ_Q are made up of branches of simple curves of the plane, and we describe what happens to the image (preimages) of a small curve segment γ when it has a tangential contact with δ_s (δ_Q) and subsequently crosses it in two points. In order to make the exposition clearer we assume, as in Sec. 2.1, that the map T has the form (3).

Consider first a bounded curve segment γ that lies entirely in a region in which no denominator of the rational map T vanishes, so that the map is continuous in all the points of γ. Since γ is a compact subset of $\Re^2$, also its image $T(\gamma)$ is compact [Fig. 6(a)]. We now imagine to move γ towards δ_s, until it becomes tangent to it in a point $A_0 = (x_0, y_0)$ which is not a focal point. This implies that the image $T(\gamma)$ is given by the union of two disjoint and unbounded branches, both asymptotic to the line σ of equation $x = F(x_0, y_0)$ [see Fig. 6(b)]. In fact, $T(\gamma) = T(\gamma_a) \cup T(\gamma_b)$, where γ_a and γ_b are the two portions of γ separated by the point $A_0 = \gamma \cap \delta_s$. In A_0 the map T is not defined and the limit of $T(x, y)$ assumes the form (7) as $(x, y) \to A_0$ along γ_a, as well as along γ_b. In such a situation any image of γ of rank $k > 1$, given by $T^k(\gamma)$, includes two disjoint unbounded branches, asymptotic to the rank-k image of the line σ, $T^k(\sigma)$.

As γ continues to move so that it crosses δ_s in two points, say $A_1 = (x_1, y_1)$ and $A_2 = (x_2, y_2)$, both nonfocal points, then the asymptote σ splits into two disjoint asymptotes σ_1 and σ_2 of equations $x = F(x_1, y_1)$ and $x = F(x_2, y_2)$ respectively, and the image $T(\gamma)$ is given by the union of three disjoint unbounded branches, $T(\gamma) = T(\gamma_a) \cup T(\gamma_c) \cup T(\gamma_b)$, where γ_a, γ_b and γ_c are the three portions of γ separated by the two points A_1 and A_2 at which the denominator vanishes. In Fig. 6(c) some different possible shapes of $T(\gamma)$ are qualitatively shown, according to the sign of the denominator $D(x, y)$ along the curve γ (i.e. whether $D(x, y)$ changes the sign or not, or whether $F(A_1)$ and $F(A_2)$ have the same sign or not). Of course, also the image of γ of rank $k > 1$, $T^k(\gamma)$, includes three disjoint unbounded arcs, asymptotic to the curves $T^k(\sigma_1)$ and $T^k(\sigma_2)$, rank-k images of σ_1 and σ_2 respectively.

The qualitative change of $T(\gamma)$, due to a contact between γ and δ_s, as described above, may represent an important contact bifurcation of a fractional map T when γ is, for example, the local unstable manifold W^u of a saddle point or saddle cycle. In fact the creation of a new unbounded branch of W^u, due to a contact with δ_s, can cause the *creation of homoclinic points*, due to new transverse intersections between the stable and unstable sets, W^s and W^u, of the same saddle point (or cycle), that do not come from a tangential contact between W^u and W^s. This implies that, in a map with denominator, homoclinic points can be created without a homoclinic tangency between W^u and W^s, due to the sudden creation of unbounded branches of W^u when it crosses δ_s. We shall see such a situation in the example of Sec. 2.3.3.

In the case of a noninvertible map, another important property, due to the presence of the curve δ_s, is expressed by the following proposition, which is a straightforward consequence of the arguments given above:

Proposition 4. *Let T be a noninvertible map of the form (3) and let LC_{-1} be the curve of merging preimages. If LC_{-1} has n transverse intersections with the set δ_s in the points $P_i = (x_i, y_i)$, $i = 1, \ldots, n$ nonfocal, then the critical set $LC = T(LC_{-1})$ includes $n + 1$ disjoint unbounded branches, separated by the n asymptotes σ_i of equation $x = F(x_i, y_i)$, $i = 1, \ldots, n$.*

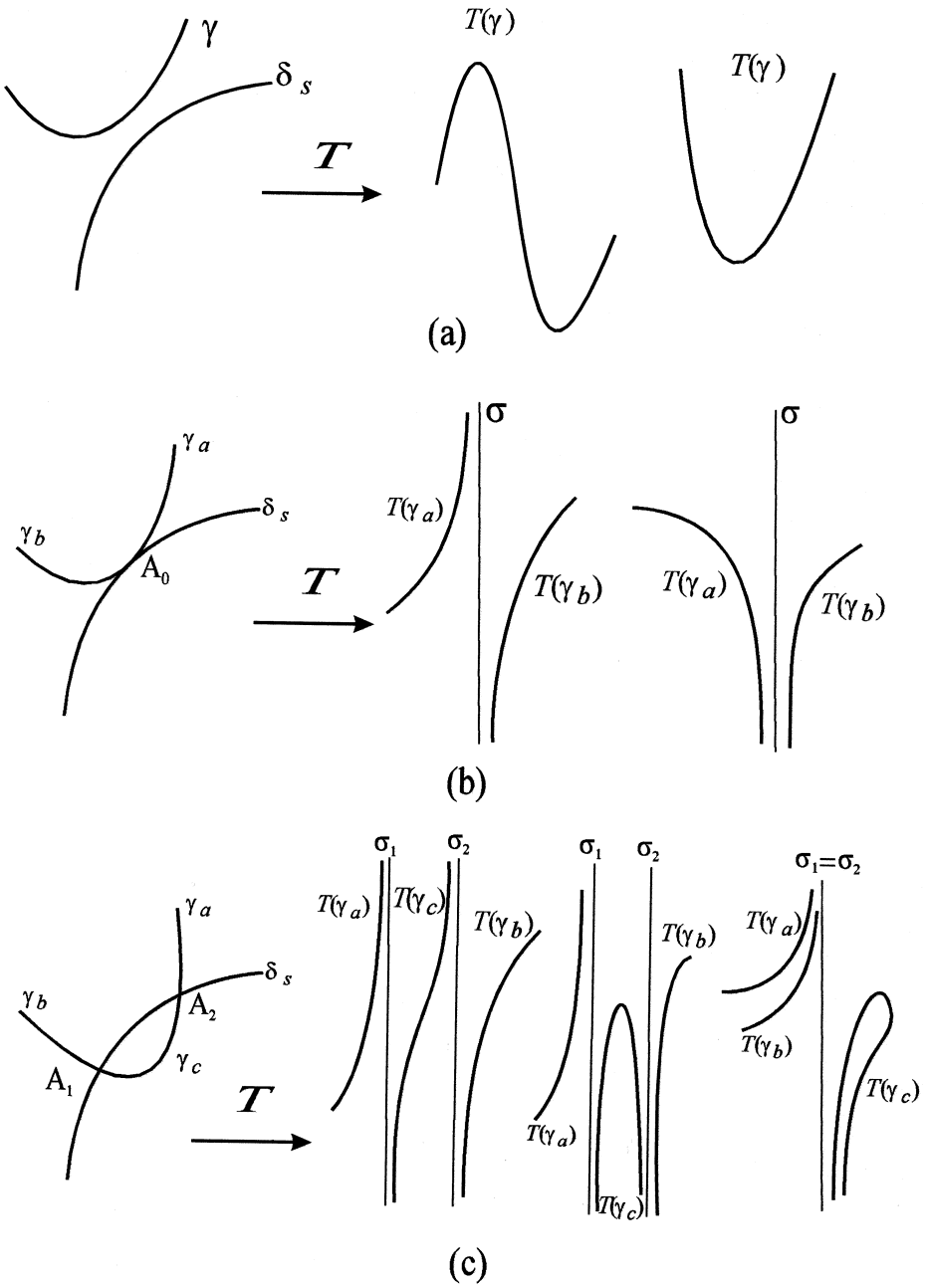

Figure 6.

We now examine the action of the inverse maps on a smooth curve segment ω that moves towards a prefocal curve δ_Q^i until it crosses δ_Q^i. Let us first consider the case of an invertible map, so that only a focal point $Q^i = T^{-1}(\delta_Q^i)$ is associated with δ_Q^i. We assume, as in the situation considered in Sec. 2.1, that δ_Q^i belongs to the line of equation $x = F(Q^i)$, and the one-to-one correspondence defined by (12) and (13) holds.

As ω moves toward δ_Q, its preimage $\omega_{-1} = T^{-1}(\omega)$ moves towards Q^i [see the qualitative sketch in Fig. 7(a)]. If ω becomes tangent to δ_Q^i in a point $C = (F(Q^i), y_c)$ then ω_{-1} has a cusp point at Q^i [Fig. 7(b)]. The slope of the common tangent to the two arcs that join in Q^i is given by $m_i(y_c)$, according to (13).

If the curve segment ω moves further, so that it crosses δ_Q^i in two points $(F(Q^i), y_1)$ and $(F(Q^i), y_2)$, then ω_{-1} forms a loop with double point at the focal point Q^i. In fact the two portions of ω that intersect δ_Q^i are both mapped by T^{-1} into arcs through Q^i, and the tangents to these two arcs

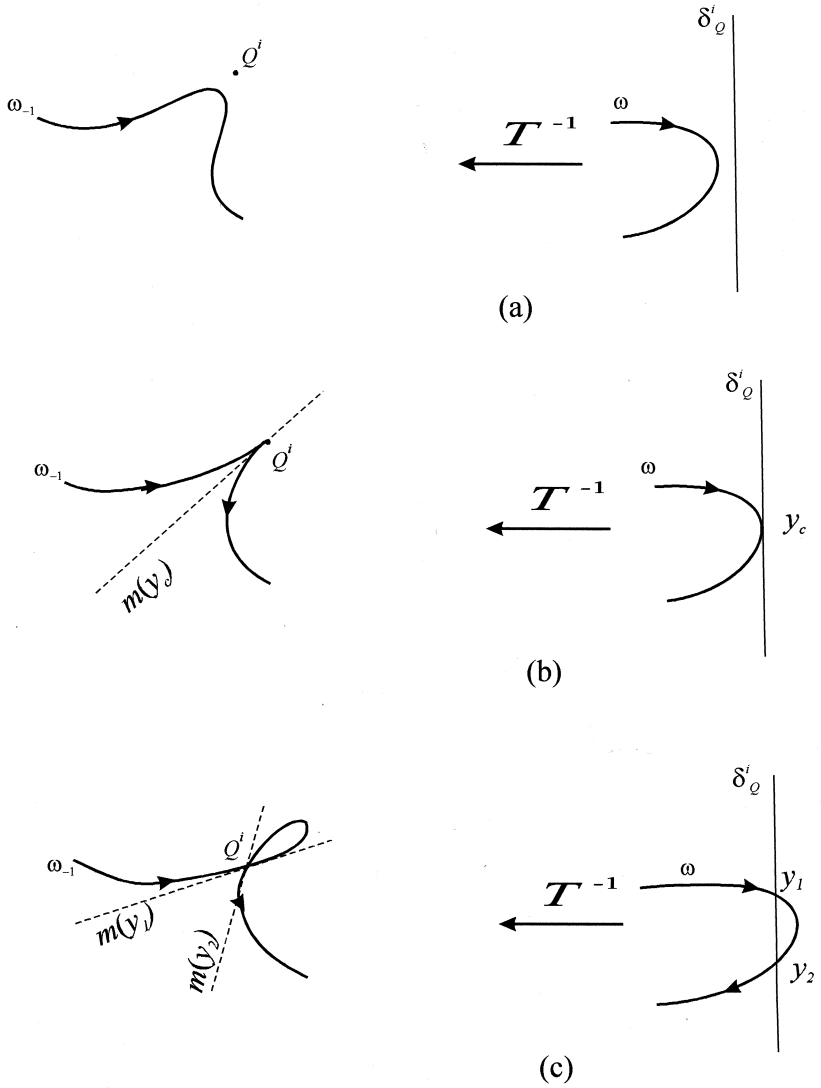

Figure 7.

of ω_{-1} issuing from the focal point have different slopes, $m_i(y_1)$ and $m_i(y_2)$ respectively, according to (13).

In the case of a noninvertible map, $k \geq 1$ distinct focal points $Q^{i,j}$, $j = 1, \ldots, k$ may be associated with a prefocal curve δ^i_Q. In this case, each inverse T_j^{-1}, $j = 1, \ldots, k$, gives a distinct preimage $\omega^j_{-1} = T_j^{-1}(\omega)$ that has a cusp point in $Q^{i,j}$, $j = 1, \ldots, k$, when the arc ω is tangent to δ^i_Q, and each preimage ω^j_{-1} has a loop in $Q^{i,j}$ when the arc ω intersects δ^i_Q in two points (see the qualitative picture of Fig. 8, that illustrates the case $k = 2$).

These qualitative changes of the shape of the preimages $T_j^{-1}(\omega)$ of an arc ω, due to a tangential contact of ω with the prefocal curve, can be particularly important for the global dynamical properties of the map T if ω is a portion of a basin boundary $\mathcal{F}$ (we shall see examples in which $\mathcal{F}$ is formed by the stable set of a saddle fixed point, or a saddle cycle, or by a repelling closed invariant curve generated by a subcritical Neimark–Hopf bifurcation). The boundary $\mathcal{F}$ of a basin is backward invariant, i.e. $T^{-1}(\mathcal{F}) = \mathcal{F}$, where here T^{-1} represents the set of all the inverses of T. Hence, if ω is a portion of $\mathcal{F}$, then all its preimages of any rank must belong to $\mathcal{F}$. This implies that if a portion ω of $\mathcal{F}$ has a contact with a prefocal curve δ^i_Q then necessarily at least k cusp points, located in the focal points $Q^{i,j}$, are included in the boundary $\mathcal{F}$. Furthermore, if the focal points $Q^{i,j}$ have preimages, then also these belong to $\mathcal{F}$, so that further cusps exist on $\mathcal{F}$, with tips at each of such preimages. From these arguments we can state that if the basin boundary $\mathcal{F}$ was smooth

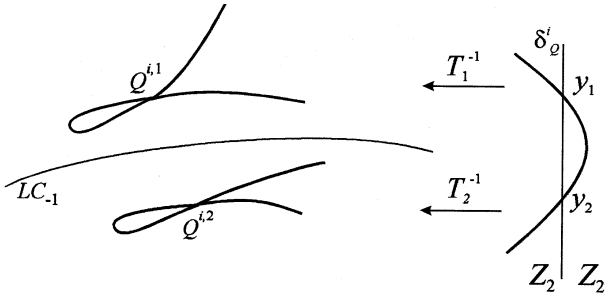

Figure 8.

before the contact with the prefocal curve δ_Q, the occurrence of such contact causes the appearance of points of nonsmoothness, that may be infinitely many if some focal point $Q^{i,j}$ has preimages of any rank.

After the contact, if a portion of the boundary $\mathcal{F}$ crosses δ_Q^i in two points, then the boundary $\mathcal{F}$ must contain at least k loops with double points in $Q^{i,j}$. Also in this case, if some focal point $Q^{i,j}$ has preimages, other loops appear (even infinitely many) with double points in the preimages of any rank of $Q^{i,j}$, $j = 1, \ldots, n$.

These arguments can be summarized by the following proposition:

Proposition 5. *A contact of a basin boundary with a prefocal curve marks the occurrence of a new type of basin bifurcation that causes the creation of cusp points and, after the crossing, of loops, along the basin boundary.*

After the first crossing between $\mathcal{F}$ and a prefocal curve δ_Q^i, that causes the creation of loops of $\mathcal{F}$ issuing from the focal point Q and its preimages (if any), other similar contact bifurcations may occur that create new lobes issuing from the same focal point. For example in [Bischi & Gardini, 1996, 1997] some examples are shown in which the first loop of $\mathcal{F}$, created by a contact between $\mathcal{F}$ and a prefocal curve δ_Q^i, grows up until it reaches δ_Q^i, so that another loop is created issuing from each focal point $Q^{i,j}$ and so on. This process may continue until infinitely many loops, issuing from each $Q^{i,j}$, are created, thus giving a very particular fractalization of the basin boundary.

It is worth noting that bifurcations of noninvertible maps, due to contacts of LC with a basin boundary, associated with the properties of maps with denominator, may give rise to new basin structures, such as those illustrated in Fig. 9. They shall be called *crescents*, obtained from the merging of lobes.

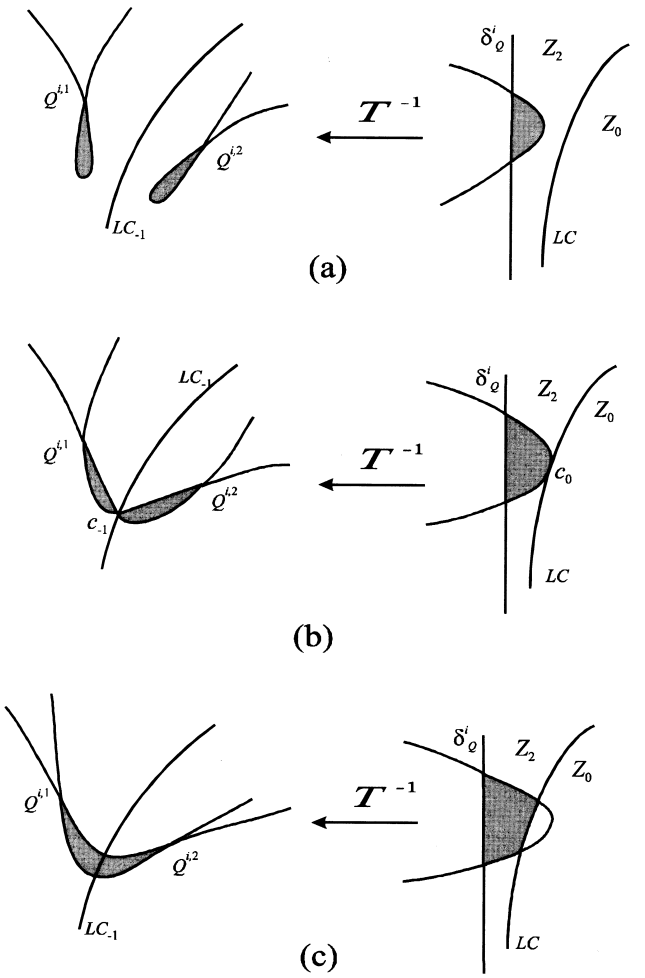

Figure 9.

Remark. The creation of "crescents", as the result of merging of lobes, is a peculiarity of noninvertible maps with denominator since it requires a contact of the boundary with a prefocal curve (located in a region with more than one inverse), at which the lobes are created, followed by a contact with a critical curve, causing the merging of the lobes. At the contact the lobes are not tangent to LC_{-1}.

2.3. *Examples*

2.3.1. *A $Z_0 - Z_2$ noninvertible map with one prefocal line*

Let us consider the map

$$T : \begin{cases} x' = y \\ y' = y - \lambda x + \dfrac{\alpha x^2 + \gamma x}{y - \beta} \end{cases} \tag{17}$$

not defined in the points of the line δ_s of equation

$$y = \beta\,. \tag{18}$$

We recall that the iteration of (17) is not defined in the preimages of δ_s as well. The map (17) is a non-invertible map of $Z_0 - Z_2$ type, i.e. a point (x', y') can have two or no preimages whose coordinates are obtained by solving the algebraic system (17) with respect to the unknowns x and y. Such system is equivalent to

$$\begin{cases} \alpha x^2 + (\gamma - \lambda(x' - \beta))x + (x' - \beta)(x' - y) = 0 \\ y = x' \end{cases} \tag{19}$$

for $y \neq \beta$, hence we have two real and distinct solutions if

$$\Delta(x', y') = (\lambda(x' - \beta) - \gamma)^2 - 4\alpha(x - \beta)(x' - y') > 0 \tag{20}$$

and no solutions if the reverse inequality holds.

The two regions Z_0 and Z_2, defined as $Z_0 = \{(x, y)|\Delta(x, y) < 0\}$ and $Z_2 = \{(x, y)|\Delta(x, y) > 0\}$, are separated by the critical curve LC, locus of points having merging preimages, defined by the equation $\Delta(x, y) = 0$, which can be expressed as

$$y = \frac{\gamma^2 + (\beta - x)(4\alpha x + 2\gamma\lambda - \lambda^2(x - \beta))}{4\alpha(\beta - x)}. \tag{21}$$

For each point $(x', y') \in Z_2$ the two rank-1 preimages are computed by the two inverse maps (obtained by solving (19))

$$T_1^{-1} : \begin{cases} x = \dfrac{1}{2\alpha}\left(\lambda(x' - \beta) - \gamma - \sqrt{\Delta(x', y')}\right) \\ y = x' \end{cases}$$

$$T_2^{-1} : \begin{cases} x = \dfrac{1}{2\alpha}\left(\lambda(x' - \beta) - \gamma + \sqrt{\Delta(x', y')}\right) \\ y = x' \end{cases}. \tag{22}$$

The map (17) has two focal points

$$Q^1 = \left(-\frac{\gamma}{\alpha}, \beta\right) \qquad \text{and} \qquad Q^2 = (0, \beta) \tag{23}$$

related to the prefocal curve δ_Q (the upper index i is not necessary in this case because only one prefocal curve exists), given by the line of equation

$$x = \beta. \tag{24}$$

For each focal point Q^i, $i = 1, 2$, the one-to-one correspondence $m_i(y)$ between slopes and points can be easily obtained from (13):

$$m_1(y) = \frac{\alpha\gamma}{\alpha(\beta - y) - \lambda\gamma} \quad \text{and} \quad m_2(y) = \frac{\gamma}{y - \beta} \tag{25}$$

for the focal points Q^1 and Q^2 respectively.

It is easy to verify that the prefocal line δ_Q is entirely included inside Z_2 and that $T_j^{-1}(\delta_Q) = Q^j$, $j = 1, 2$. The critical set LC is formed by two branches with the prefocal curve as a vertical asymptote (so that LC does not intersect it, as stated in Proposition 2). The merging preimages of the points belonging to LC are located on the line of equation

$$y = \frac{2\alpha}{\lambda}x + \frac{\gamma}{\lambda} + \beta \tag{26}$$

which constitutes the curve LC_{-1} of merging preimages. In this example the locus LC_{-1} can also be obtained from the condition $\det(DT(x, y)) = 0$, where DT denotes the Jacobian matrix of the map T. It is worth noticing that, according to Proposition 4, LC is made up of two disjoint unbounded branches (asymptotic to the line $x = \beta$) because $\overline{LC_{-1}}$ intersects the line δ_s in a point which is not focal.

The map (17) has two fixed points:

$$O = (0, 0) \qquad \text{and} \qquad P = \left(\frac{\lambda\beta + \gamma}{\lambda - \alpha}, \frac{\lambda\beta + \gamma}{\lambda - \alpha}\right). \tag{27}$$

For the parameter values $\alpha = 0.499$, $\gamma = 0.5$, $\beta = \sqrt{2}$, $\lambda = -0.75$, the fixed point P is a stable focus and the fixed point O is a saddle. In Fig. 10 the basin of attraction $\mathcal{B}(P)$ of the attracting fixed point is represented by the red region, whereas the grey region represents the basin of infinity, i.e. the set of points that generate diverging trajectories. In Fig. 10 also the critical curve LC and the curve LC_{-1} of merging preimages are represented.

For the set of parameters of Fig. 10 the basin $\mathcal{B}(P)$ is a simply connected region with a smooth boundary $\partial\mathcal{B}(P)$. This boundary is formed by the stable set $W^s(O)$ of the saddle point O. If we denote by W^s_{loc} the arc $B_{-1}B$ of the stable manifold of O, where $B_{-1} \in LC_{-1}$, $B \in LC$ and O belongs to the arc $B_{-1}B$, then we have $W^s(O) = \partial\mathcal{B}(P) = \bigcup_{k=1}^{3} T^{-k}(W^s_{\text{loc}})$, where $T^{-1}(\cdot) = T_1^{-1}(\cdot) \cup T_2^{-1}(\cdot)$. In fact, the rank-1 preimage of the saddle O, different from O, denoted by O_{-1} in Fig. 10, belongs to the region Z_2, and its two rank-1 preimages, denoted by $O^{(1)}_{-2}$ and $O^{(2)}_{-2}$, are both located in the region Z_0, so

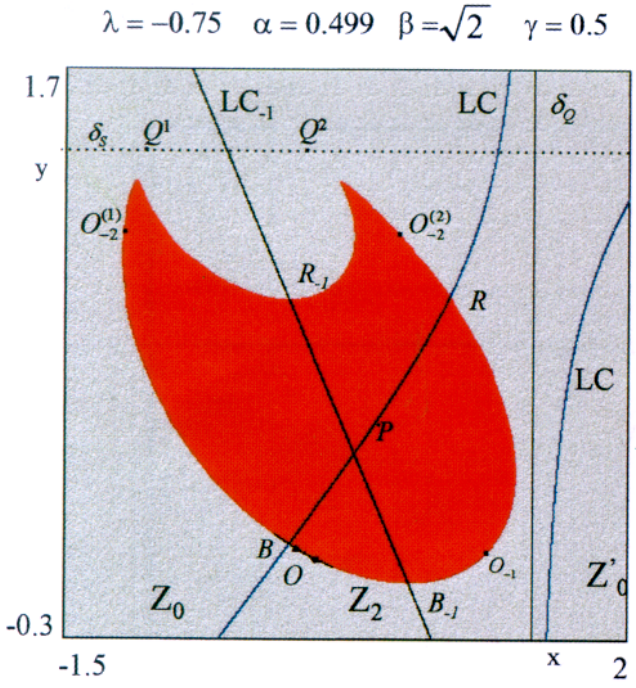

Figure 10.

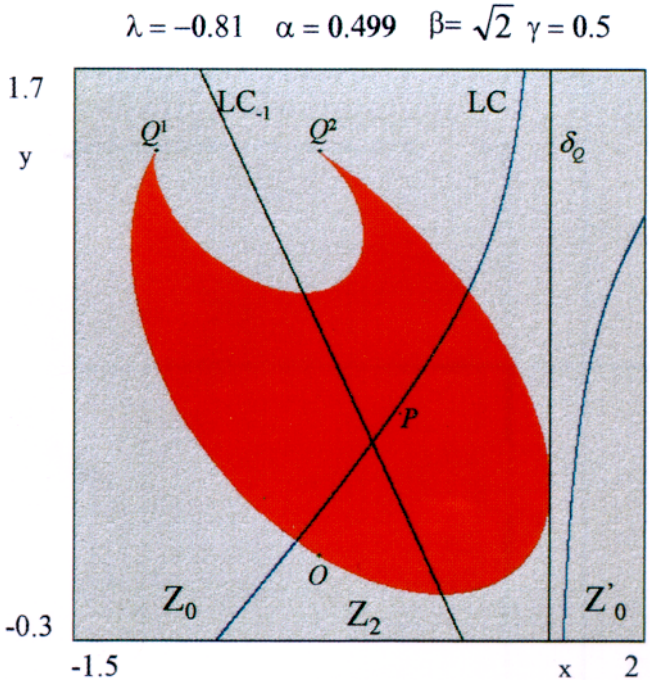

Figure 11.

that no preimages of O of rank greater than 2 exist. This completes the smooth boundary, as shown in Fig. 10.

We now describe how the boundary $\partial\mathcal{B}(P)$ of the basin of the stable fixed point P changes as the parameter λ varies. If λ decreases, a portion of $\partial\mathcal{B}(P)$ approaches the prefocal line δ_Q, and consequently two other portions of $\partial\mathcal{B}(P)$ approach the two focal points Q^1 and Q^2. At $\lambda = -0.81\ldots$ $\partial\mathcal{B}(P)$ has a contact with δ_Q, and consequently two cusp points are created on $\partial\mathcal{B}(P)$, with vertexes in Q^1 and Q^2 (Fig. 11). Hence the contact between $\partial\mathcal{B}(P)$ and the prefocal curve causes a bifurcation at which the basin boundary is changed from smooth to nonsmooth, according to Proposition 5.

As λ is further decreased, $\partial\mathcal{B}(P)$ crosses the prefocal line in two points (Fig. 12). This implies that the two preimages of this portion are two loops with double points in the focal points, according to the arguments given in Sec. 2.2. These two loops of $W^s(O)$ bound two lobes of the red basin issuing from the focal points, clearly visible in Fig. 12.

We remark that this is a new bifurcation of the basin boundary, due to the presence of the prefocal curve. After the bifurcation, the basin $\mathcal{B}(P)$ ought to be called "nonconnected" since the focal points do not belong to the domain of the map T. However we believe that it is more convenient to call

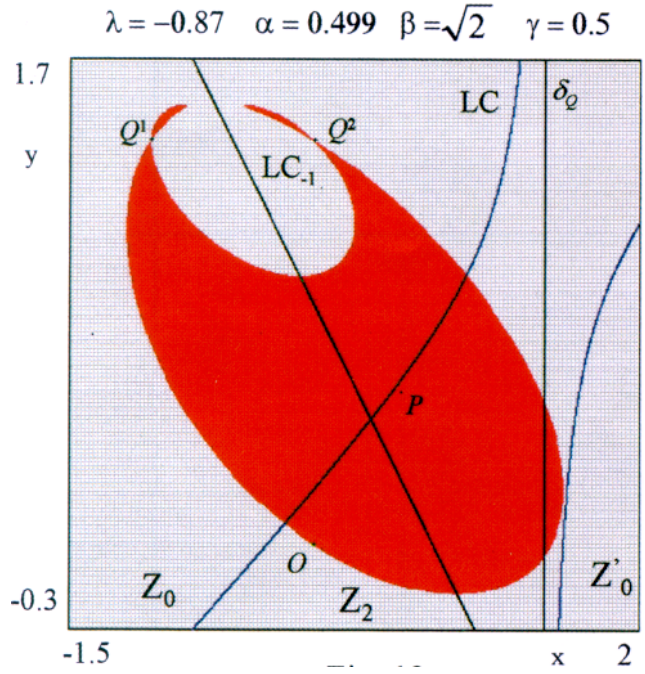

Figure 12.

such a basin connected through focal points due to the fact that its closure $\overline{\mathcal{B}(P)}$ is connected.

Just after the bifurcation the two lobes issuing from Q^1 and Q^2 are disjoint, being the two distinct preimages of the portion of $\mathcal{B}(P)$ located on the right of δ_Q. As λ is further decreased, that portion moves towards LC and at $\lambda = \lambda_c$, with

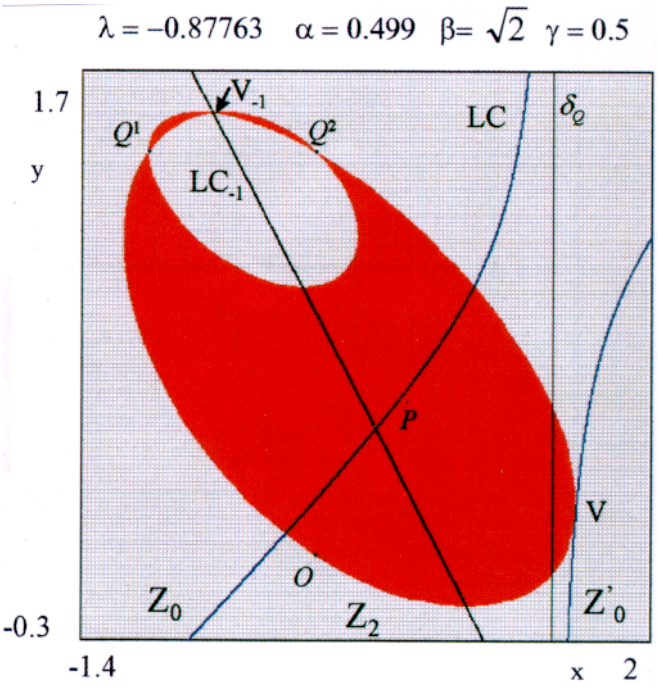

Figure 13.

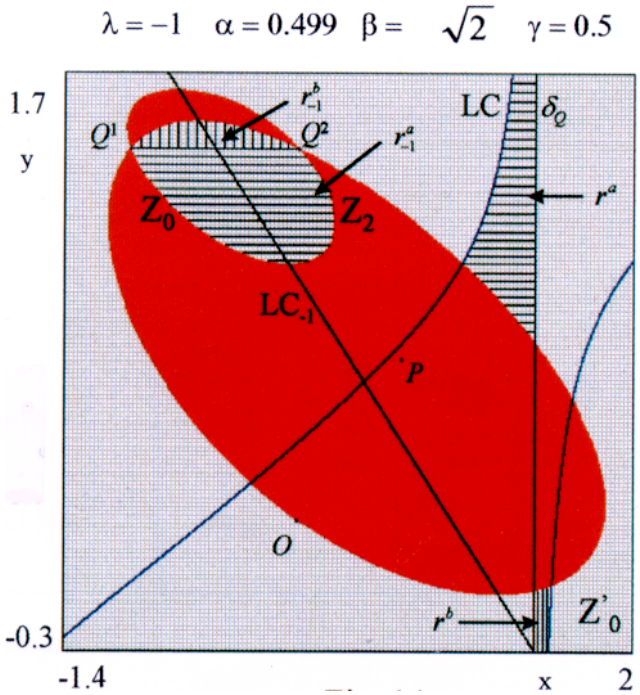

Figure 14.

$\lambda_c \simeq -0.87763$, $\partial\mathcal{B}(P)$ has a contact with the critical curve LC in a point V. At this contact the two lobes merge, i.e. they have a common point V_{-1} located on LC_{-1} (Fig. 13). This point is given by the merging preimages of the contact point V between LC and $\partial\mathcal{B}(P)$. This is a well known contact bifurcation of noninvertible maps [Mira *et al.*, 1994; Mira *et al.*, 1996]. We remark that at the bifurcation the contact between the two lobes in the point V_{-1} of LC_{-1} is not smooth, i.e. the common tangent does not exist (see [Mira *et al.*, 1996]).

After this bifurcation the two lobes issuing from Q^1 and Q^2 merge and form a unique *crescent* connecting the two focal points (Fig. 14), as explained at the end of Sec. 2.2. We remark again that the creation of a crescent is due both to the presence of the focal points and to the presence of LC, i.e. to the existence of a prefocal curve together with the noninvertibility of the map. It represents here a new basin bifurcation that marks the transition of $\overline{\mathcal{B}(P)}$ from a simply connected set to a multiply connected one, or, equivalently, the transition of the basin of infinity from connected to nonconnected, due to the creation of the disjoint "island" nested inside $\overline{\mathcal{B}(P)}$. After the bifurcation $\overline{\mathcal{B}(P)}$ has an annular structure, made up of two parts joined by the focal points, as in Fig. 14, obtained for $\lambda = -1$. It is worth to note that the portion of the basin of infinity nested inside $\mathcal{B}(P)$ is made up of two bounded regions, located at opposite sides with respect to δ_s, given by the preimages of the two unbounded portions of the basin of infinity, belonging to the region Z_2, located between LC and δ_Q (these portions, and their bounded preimages, are represented by the hatchured regions in Fig. 14). The fact that the preimages of unbounded regions are bounded is due to the particular properties of the prefocal curve.

Another interesting situation is obtained for the parameter values $\lambda = -0.8$, $\gamma = -0.18$, $\beta = \sqrt{2}$ and $\alpha = 0.54$. For this set of parameters the fixed point P is a repelling focus and a chaotic attractor exists around it [represented by the black points in Fig. 15(a)]. The basin of bounded iterated sequences (which includes this attractor), represented by the red region in Fig. 15(a), is separated from the basin of infinity by the stable set of the saddle fixed point O. It can be noticed that the portion H_0 of the basin of infinity, indicated by the arrow in Fig. 15(a), has crossed LC entering the region Z_2 [see also the enlargement in Fig. 15(b)]. The two preimages of this portion constitute a "hole" of the basin of infinity (or "lake", following the terminology introduced in [Mira *et al.*, 1994]) nested inside the red basin. This is a well known contact bifurcation, typical of noninvertible maps (see [Mira *et al.*, 1994; Mira *et al.*, 1996, Chap. 5; Abraham *et al.*, 1997, Chap. 5]). The "main hole", denoted by

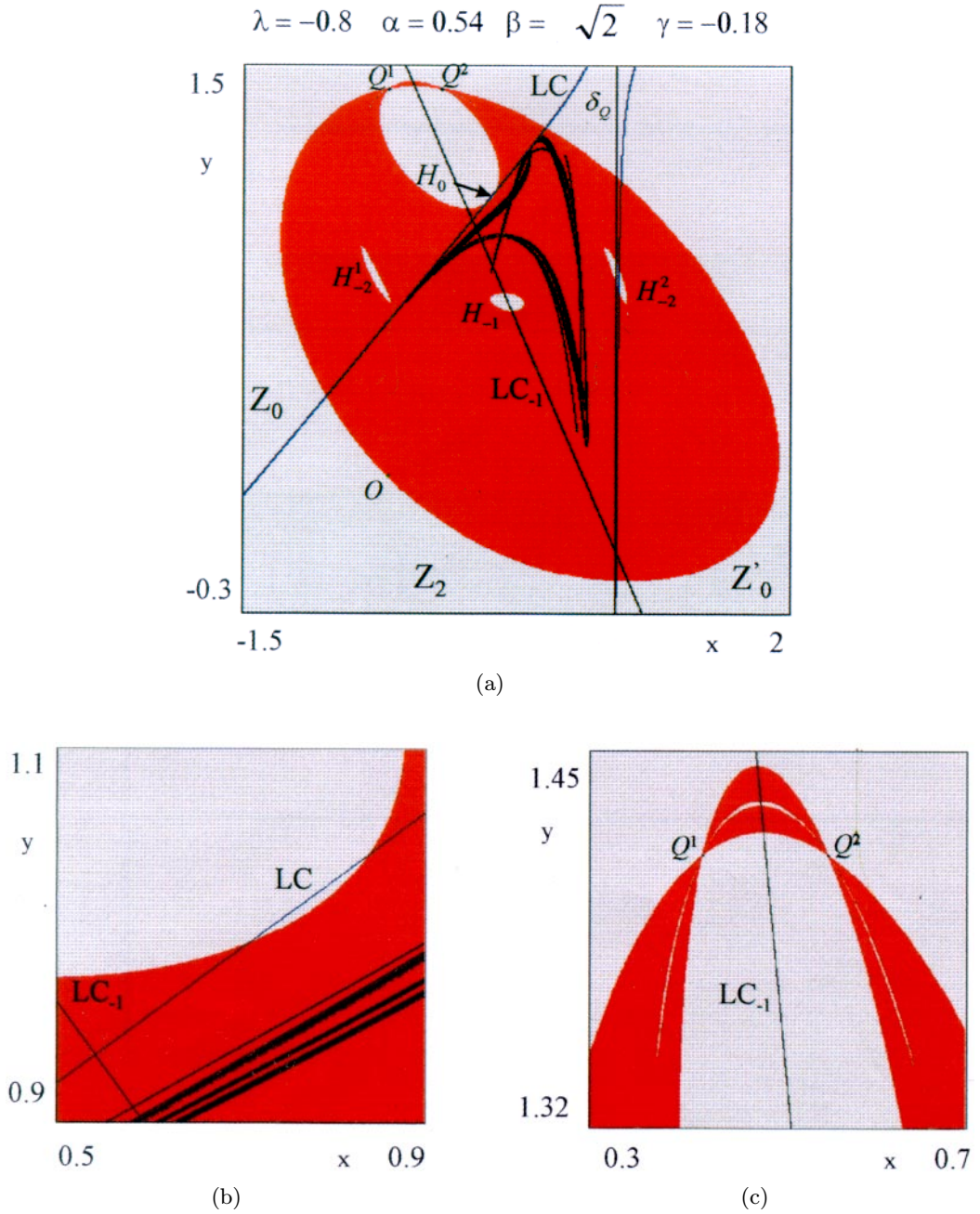

Figure 15.

H_{-1} in Fig. 15(a), is entirely included in the region Z_2, hence it has two rank-one preimages, denoted by H^1_{-2} and H^2_{-2} in Fig. 15(a). One of these, H^1_{-2}, belongs to Z_0 , whereas the other one is partially included inside the region Z_2, and crosses both δ_Q and LC. Its preimages form a grey "crescent" and two lobes issuing form the focal points, more clearly visible in the enlargement shown in Fig. 15(c). The basin structure shown in Fig. 15(a) is specific to a noninvertible map with denominator.

Figure 16, which corresponds to the parameters $\alpha = 0.537$, $\beta = \sqrt{2}$, $\gamma = -0.18$ and $\lambda = -0.8$, gives an interesting situation. The first homoclinic bifurcation of the saddle fixed point O is near to occur. The chaotic attractor (represented in black) is near its basin boundary, and the homoclinic bifurcation is due to a contact of the boundary of the chaotic area with the boundary of its basin of attraction, leading to the destruction of the chaotic attractor [Gumowski & Mira, 1978, 1980],

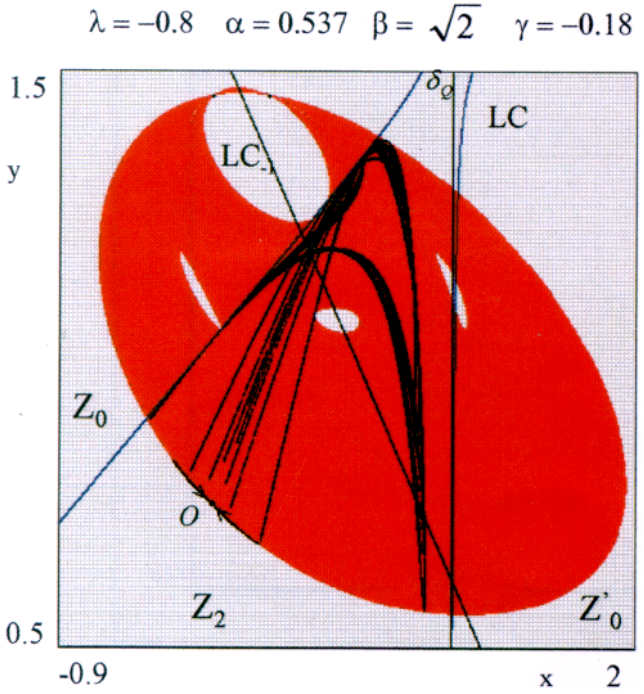

Figure 16.

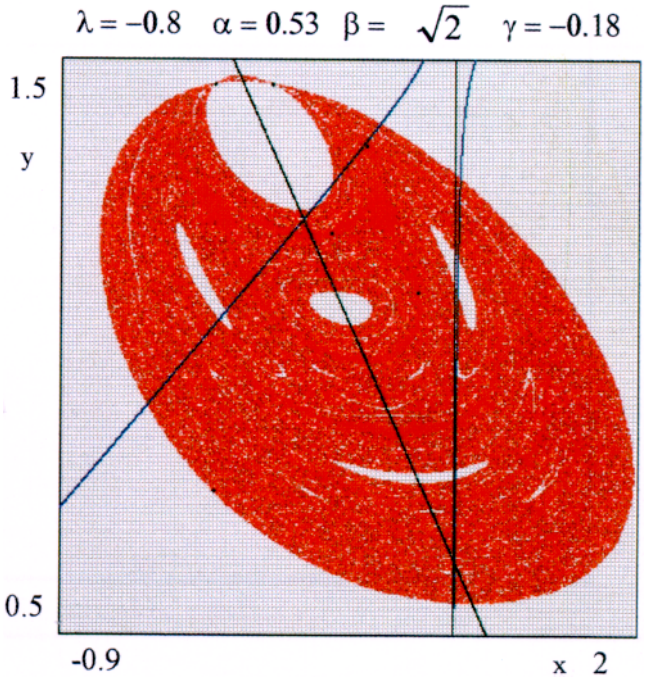

Figure 17.

a situation called *final bifurcation* in [Mira *et al.*, 1996; Abraham *et al.*, 1997] or *boundary crisis* in [Grebogi *et al.*, 1983].

The contact bifurcation occurs at $\alpha \simeq 0.53648$, the other parameters being the same as above. This bifurcation gives rise to a fractal structure of the basin $\mathcal{B}$ of bounded orbits, given by the red region of Fig. 17, obtained for $\alpha = 0.53$. At this parameter value infinitely many lakes, arborescent sequence of the increasing rank preimages of H_0, exist, and infinitely many of them cross through the prefocal curve, thus creating infinitely many lobes of lakes crossing through the two focal points. It can be noticed that at this stage the basin $\mathcal{B}$ of bounded iterated sequences contains a period three stable cycle of focus type, represented by black dots in Fig. 17, and other coexisting attractors may exist. The boundary $\partial\mathcal{B}$ includes a strange repeller: the fractal set of the unstable cycles of the former chaotic attractor, as well as their stable sets and all their limit points.

2.3.2. *A $Z_0 - Z_2$ noninvertible map with two prefocal lines*

Let us consider the map

$$T : \begin{cases} x' = y \\ y' = y - \lambda x + \dfrac{\alpha x^2 + \gamma x}{(y - \beta_1)(y - \beta_2)} \end{cases} \tag{28}$$

not defined in the points of the set $\delta_s = \delta_s^1 \cup \delta_s^2$, where δ_s^1 and δ_s^2 are the lines of equation

$$y = \beta_1 \qquad \text{and} \qquad y = \beta_2 \tag{29}$$

respectively. The map T is a noninvertible map of $Z_0 - Z_2$ type. In fact, the preimages of a point (x', y') are the real solutions of the second degree algebraic system

$$\begin{cases} \alpha x^2 + (\gamma - \lambda(x' - \beta))x + (x' - \beta)(x' - y') = 0 \\ y = x' \end{cases} \tag{30}$$

equivalent to the system (28) for $y \neq \beta_1$ and $y \neq \beta_2$. Hence a point (x', y') has two distinct preimages if

$$\begin{aligned} &\Delta(x', y') \\ &\quad = (\lambda(x' - \beta_1)(x' - \beta_2) - \gamma)^2 \\ &\qquad - 4\alpha(x' - \beta_1)(x' - \beta_2)(x' - y') > 0 \end{aligned} \tag{31}$$

and no preimages if the reverse inequality holds.

If the point $(x', y') \in Z_2$ then the two rank-1 preimages are computed by the two inverse

maps

$$T_1^{-1}: \begin{cases} x = \dfrac{1}{2\alpha}(\lambda(x'-\beta_1)(x'-\beta_2) \\ \qquad -\gamma - \sqrt{\Delta(x',\, y')}) \\ y = x' \end{cases} \tag{32}$$

$$T_2^{-1}: \begin{cases} x = \dfrac{1}{2\alpha}(\lambda(x'-\beta_1)(x'-\beta_2) \\ \qquad -\gamma + \sqrt{\Delta(x',\, y')}) \\ y = x' \end{cases} .$$

The critical curve LC, defined by the equation $\Delta(x, y) = 0$, can be expressed as

$$y = \frac{4\alpha x(x-\beta_1)(x-\beta_2) - (\lambda(x-\beta_1)(x-\beta_2)-\gamma)^2}{4\alpha(x-\beta_1)(x-\beta_2)} . \tag{33}$$

The map (28) has two focal points

$$Q^{1,1} = \left(-\frac{\gamma}{\alpha},\, \beta_1\right); \quad Q^{1,2} = (0,\, \beta_1) \tag{34}$$

related to the prefocal line δ_Q^1 of equation

$$x = \beta_1 \tag{35}$$

and

$$Q^{2,1} = \left(-\frac{\gamma}{\alpha},\, \beta_2\right); \quad Q^{2,2} = (0,\, \beta_2) \tag{36}$$

related to the prefocal line δ_Q^2 of equation

$$x = \beta_2 . \tag{37}$$

Both the prefocal lines are entirely included inside the region Z_2, and it is easy to verify that $T_j^{-1}(\delta_Q^i) = Q^{i,j}$, $i = 1, 2$, $j = 1, 2$. The curve LC_{-1} of merging preimages is given by the parabola of equation

$$x = \frac{\lambda}{2\alpha}[(y-\beta_1)(y-\beta_2) - \gamma] \tag{38}$$

deprived of its intersections with δ_s^1 and δ_s^2. According to Proposition 4, the critical set LC is made up of three disjoint unbounded branches, because LC_{-1} crosses the set δ_S in two points which are not focal, belonging to δ_s^1 and δ_s^2 respectively (see Fig. 18).

For each focal point $Q^{i,j}$, $i, j = 1, 2$, the one-to-one correspondence $m_{i,j}(y)$ between slopes and

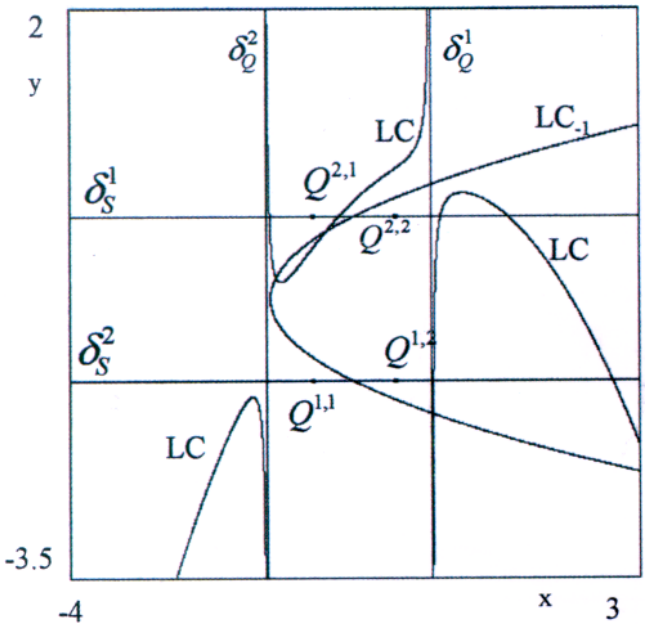

Figure 18.

points can be easily obtained from (13)

$$\begin{aligned} m_{1,1}(y) &= \frac{\alpha\gamma}{(\beta_1-\beta_2)(\alpha\beta_1+\lambda\gamma-\alpha y)}; \\ m_{1,2}(y) &= \frac{\gamma}{(\beta_1-\beta_2)(y-\beta_1)} \\ m_{2,1}(y) &= \frac{\alpha\gamma}{(\beta_2-\beta_1)(\alpha\beta_2+\lambda\gamma-\alpha y)}; \\ m_{2,2}(y) &= \frac{\gamma}{(\beta_2-\beta_1)(y-\beta_2)} . \end{aligned} \tag{39}$$

The origin $O = (0, 0)$ is a fixed point of (28) and other fixed points, say E and P, exist if the following second degree algebraic system

$$\begin{cases} y = x \\ \lambda x^2 - ((\beta_1+\beta_2)\lambda+\alpha)x + \lambda\beta_1\beta_2 - \gamma = 0 \end{cases} \tag{40}$$

has real solutions.

We consider the parameter values $\alpha = 0.5$, $\beta_1 = \sqrt{0.2}$, $\beta_2 = -\sqrt{2.5}$, $\gamma = 0.5$ and $\lambda = 1$. The fixed point O is an unstable focus, and the second fixed point P is a saddle. The red region shown in Fig. 19 is the basin of bounded iterated sequences, and contains a chaotic area, represented by the black points, around the saddle point P. For this set of parameters three focal points are in the Z_2 regions, i.e. they generate chains of arborescent preimages of increasing rank. One of the focal points, $Q^{2,1}$, is located in Z_0, so that it has no preimages. These chains of preimages explain the complexity of the basin

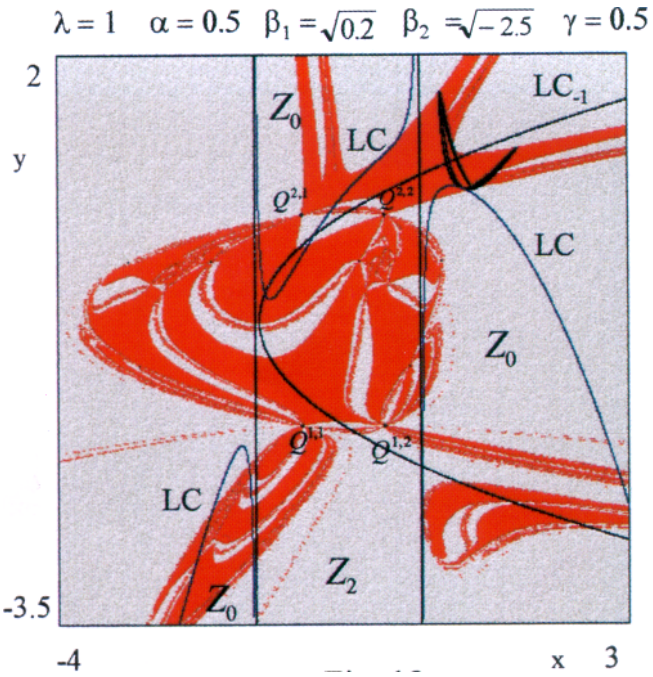

Figure 19.

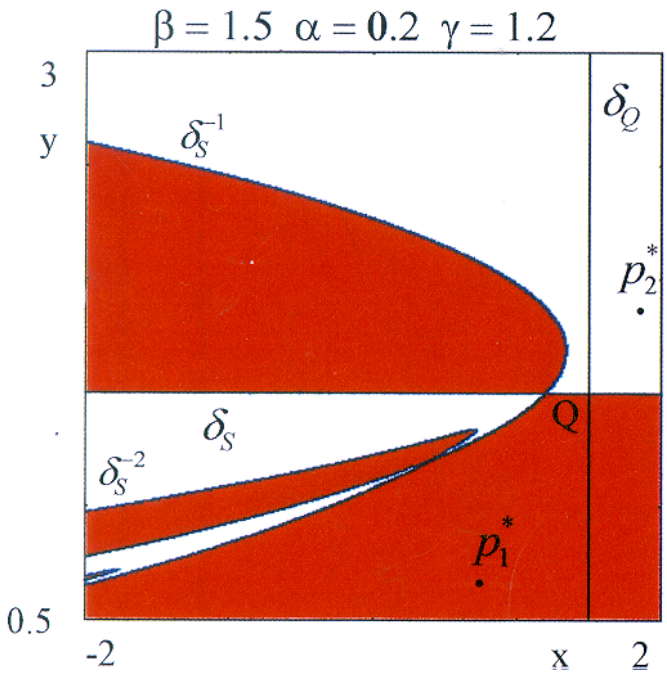

Figure 20.

structure. Simpler basins are obtained when less focal points are in Z_2.

2.3.3. *An invertible map with one prefocal line*

The map

$$T : \begin{cases} x' = y \\ y' = (1-\alpha)y + \alpha\dfrac{x-\gamma}{y-\beta} \end{cases} \tag{41}$$

is not defined in the points of the line δ_s of equation

$$y = \beta \tag{42}$$

on which the focal point

$$Q = (\gamma, \beta) \tag{43}$$

exists, with prefocal curve δ_Q of equation

$$x = \beta\,. \tag{44}$$

The relations (12) and (13), that define the one-to-one correspondence $m \leftrightarrow (\beta, y)$, between slopes of arcs through Q and points of δ_Q, become, respectively,

$$y(m) = (1-\alpha)\beta + \frac{\alpha}{m}$$

and

$$m(y) = \frac{\alpha}{y-(1-\alpha)\beta}\,. \tag{45}$$

If $(\beta+1)^2 - 4\gamma > 0$ the map (41) has two fixed points, solutions of the system

$$\begin{cases} x^2 - (\beta+1)x + \gamma = 0 \\ x = y\,. \end{cases} \tag{46}$$

Notice that the two fixed points do not depend on the parameter α. In order to show, for the map (41), some peculiar bifurcations of the basin boundaries we fix the parameters $\beta = 1.5$ and $\gamma = 1.2$, so that the fixed points are $P_1^* = (0.648\ldots, 0.648\ldots)$ and $P_2^* = (1.852\ldots, 1.852\ldots)$, and we vary the parameter α. At $\alpha = 0.2$, P_1^* is a stable focus and P_2^* is a stable node. These two coexisting attracting fixed points are shown in Fig. 20, where the respective basins of attraction $\mathcal{B}(P_1^*)$ and $\mathcal{B}(P_2^*)$ are represented by the red and white regions respectively.

The boundary that separates the two basins, say $\mathcal{F} = \partial\mathcal{B}(P_1^*) = \partial\mathcal{B}(P_2^*)$, is formed by the line of nondefinition δ_s and its preimages:

$$\mathcal{F} = \bigcup_{k=0}^{\infty} T^{-k}(\delta_s).$$

The fact that the line δ_s, at which the denominator vanishes, belongs to the boundary that separates the two basins of attraction is a peculiar property of maps with denominator. We remark that in this case no saddles nor repelling nodes exist, hence the boundary of the domain of definition of T is also the boundary which separates the basins. The

preimages of δ_s can be easily obtained by inverting the map (41), i.e. by expressing the variables x and y in terms of x' and y'. Such inverse map is given by

$$T^{-1}: \begin{cases} x = \dfrac{\beta(1-\alpha)}{\alpha}x' - \dfrac{1-\alpha}{\alpha}x'^2 \\ \qquad + \dfrac{1}{\alpha}x'y' - \dfrac{\beta}{\alpha}y' + \gamma \\ y = x' \end{cases} \tag{47}$$

provided that $y \neq \beta$, i.e. $x' \neq \beta$ according to the first of (41). From (47) with $y' = \beta$ we obtain that the rank-1 preimages of the points of δ_s are located on the parabola δ_s^{-1} of equation

$$x = \frac{\alpha-1}{\alpha}y^2 + \beta\left(\frac{2}{\alpha} - 1\right)y + \gamma - \frac{\beta^2}{\alpha} \tag{48}$$

i.e. points belonging to the parabola (48) are mapped by T into points of the line δ_s. This parabola is clearly visible in Fig. 20. Preimages of δ_s of rank $k > 1$, i.e. the sets of points that are mapped into the singular line after k iterations of the map (41), can be obtained by a similar procedure, even if their analytical expressions becomes more and more complicated. The line δ_s, its preimage δ_s^{-1} and some higher rank preimages δ_s^{-k} are represented by blue curves in Fig. 20, and they clearly appear to be located on the boundary that separates the red and white regions, that is, the numerically obtained basins of attraction of the stable fixed points P_1^* and P_2^* respectively.

As the parameter α increases, the vertex V of the parabola (48) moves to the right and at $\alpha = \alpha_b$, where $\alpha_b = 4(\beta-\gamma)/(\beta^2 + 4(\beta-\gamma)) \simeq 0.3478$, the parabola δ_s^{-1} is tangent to the prefocal line (44) in the point $V_b = (\beta, y_b)$, with $y_b = 0.5\beta(2-\alpha)/(1-\alpha) \simeq 1.899$. This implies that its preimage δ_s^{-2} has a cusp with tip on the focal point Q and tangent of slope $m_b = 2(1-\alpha)/\beta(3-2\alpha) \simeq 0.377$ (Fig. 21), according to the second of Eqs. (45) with $y = y_b$.

This first contact between the basin boundary $\mathcal{F}$ and the prefocal line δ_Q represents a global bifurcation at which the first loop of $\mathcal{F}$, bounding a lobe of $\mathcal{B}(P_1^*)$, is created. In fact, for $\alpha > \alpha_b$, just after the bifurcation, δ_s^{-2} has a loop with double point in Q, the slopes of the two tangents to δ_s^{-2} in Q being given by the two values of m obtained by the relation (45) with the y coordinates of the two intersections of the parabola δ_s^{-1} with the prefocal

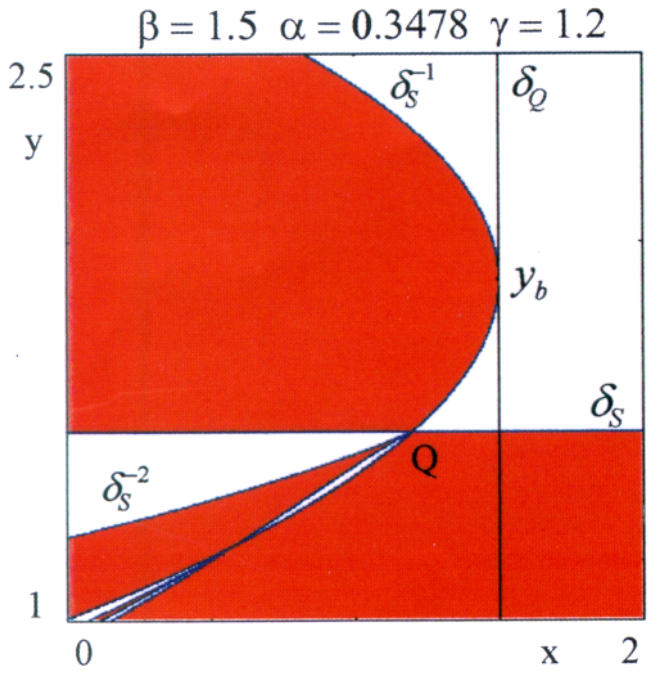

Figure 21.

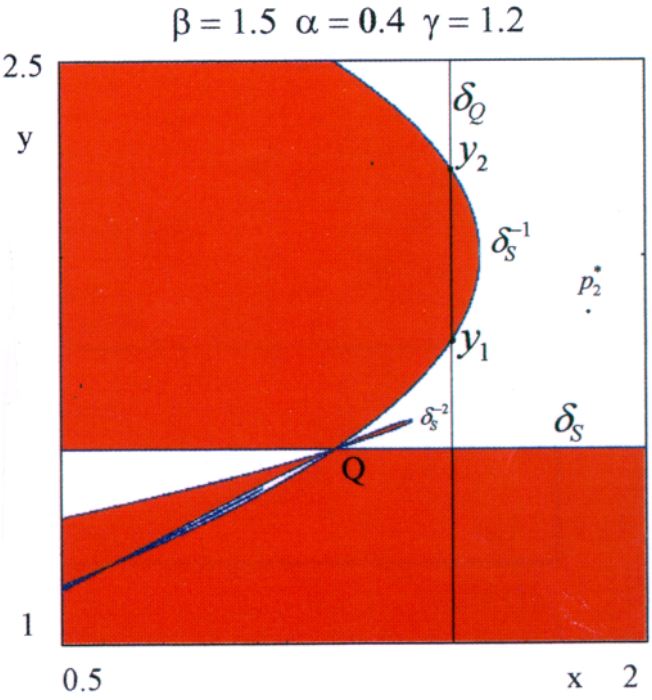

Figure 22.

line, denoted by y_1 and y_2 in Fig. 22. The lobe of $\mathcal{B}(P_1^*)$, issuing from the focal point, is clearly visible in Fig. 22, obtained with $\alpha = 0.4$. For the set of parameters used in Figs. 21 and 22, the trajectories starting in the white region converge to a stable cycle of period 2 (not visible in the figure) created at $\alpha \cong 0.2198$ through a flip bifurcation at which the

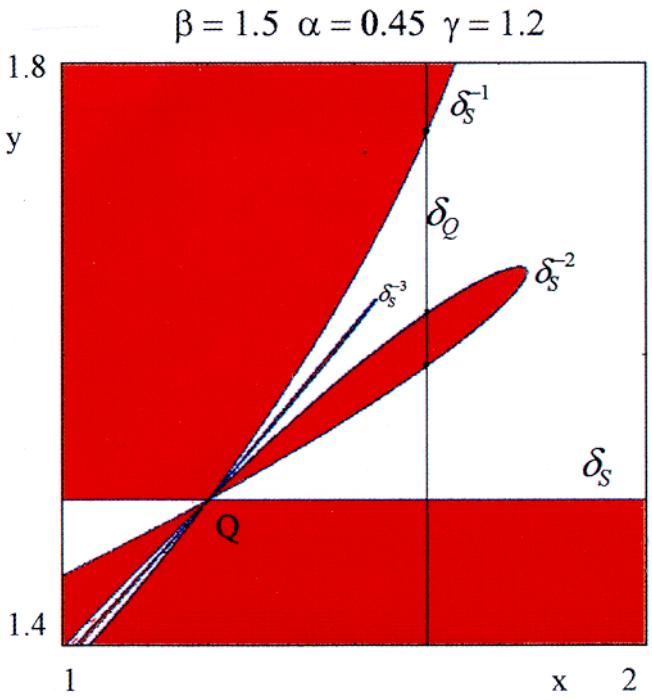

Figure 23.

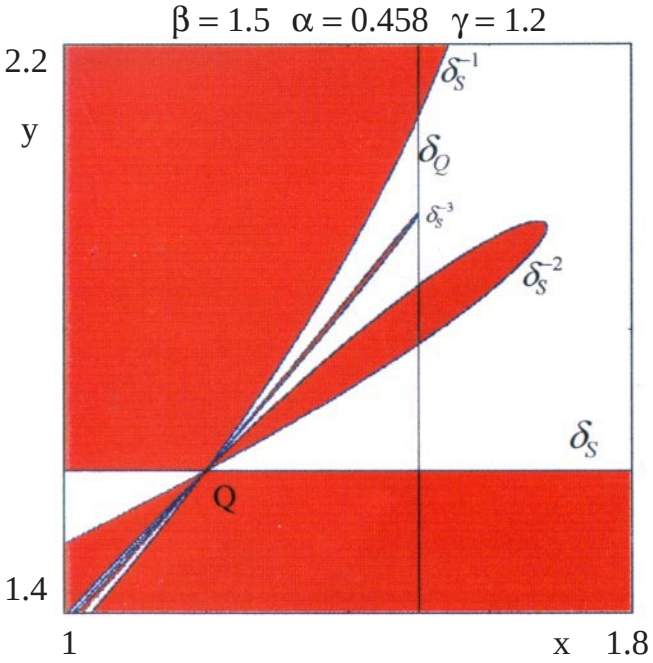

Figure 24.

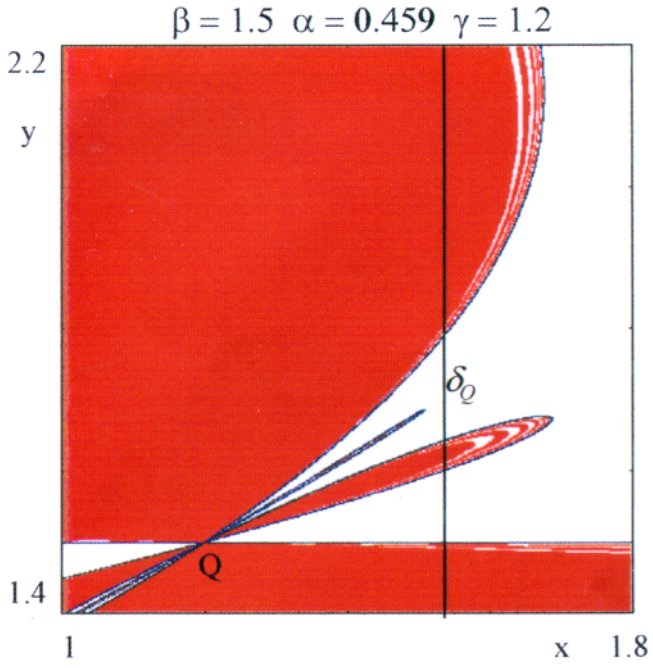

Figure 25.

fixed point P_2^* is changed from a stable node to a saddle point.

As the parameter α is further increased the x coordinate of the vertex V of δ_s^{-1} continues to increase, and the same is true for its preimages. This implies that also the lobe bounded by δ_s^{-2} moves toward the prefocal curve δ_Q, and another bifurcation value of the parameter α exists, say α_b^1, at which this lobe has a contact with the prefocal curve. For $\alpha = \alpha_b^1$ the curve δ_s^{-3} reaches the focal point Q and has a cusp in it, with slope $m_b^1 > m_b$, since the y coordinate of the contact between δ_s^{-2} and δ_Q is less than y_b. This implies that for $\alpha > \alpha_b^1$ another lobe of the basin $\mathcal{B}(P_1^*)$ is created, bounded by a loop of δ_s^{-3} located between the parabola δ_s^{-1} and the lobe bounded by δ_s^{-2} (see Fig. 23). As α increases, the creation of a new lobe issuing from the focal point Q occurs at each contact of an old lobe with the prefocal line δ_Q (as in Fig. 24, where for $\alpha = 0.458$ the lobe bounded by δ_s^{-3} is tangent to δ_Q, so that a cusp of δ_s^{-4} is ready to give a new lobe issuing from Q).

At $\alpha = \alpha_c$, with $\alpha_c = 0.4583936\ldots$, another bifurcation occurs that causes a sudden change in the structure of the basins, due to the creation of white crescents inside the red lobes (see Fig. 25). Also the bifurcation that leads to this new basin structure can be characterized by contacts between the basin boundary $\mathcal{F}$, i.e. a preimage of the singular line δ_s, and the prefocal line δ_Q. In fact, white lobes issuing from Q, and nested inside the red basin $\mathcal{B}(P_1^*)$, are created whenever a white tongue of $\mathcal{B}(P_2^*)$ crosses δ_Q. The bifurcation value α_c corresponds to the value of α at which the first tongue, bounded by a preimage δ_s^{-k} of δ_s, has a contact with δ_Q. In Fig. 26, obtained with $\alpha = 0.4583938$, i.e. just after the bifurcation value, four "white tongues",

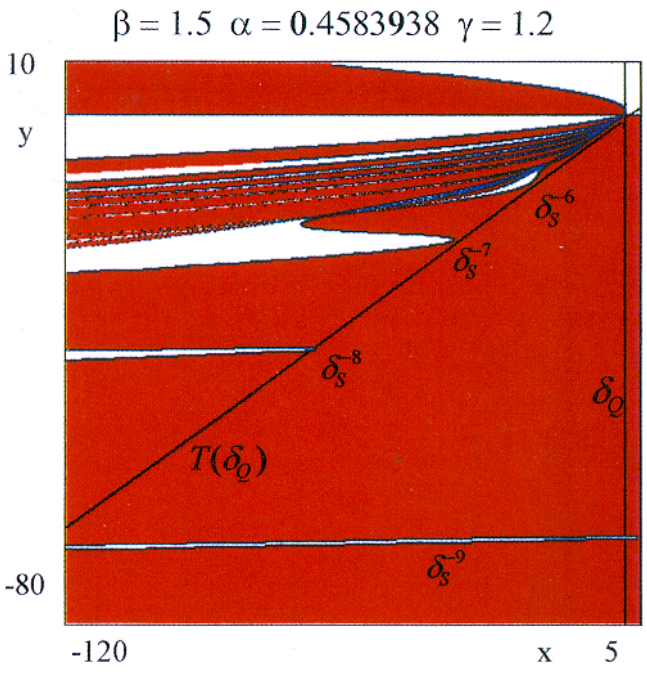

Figure 26.

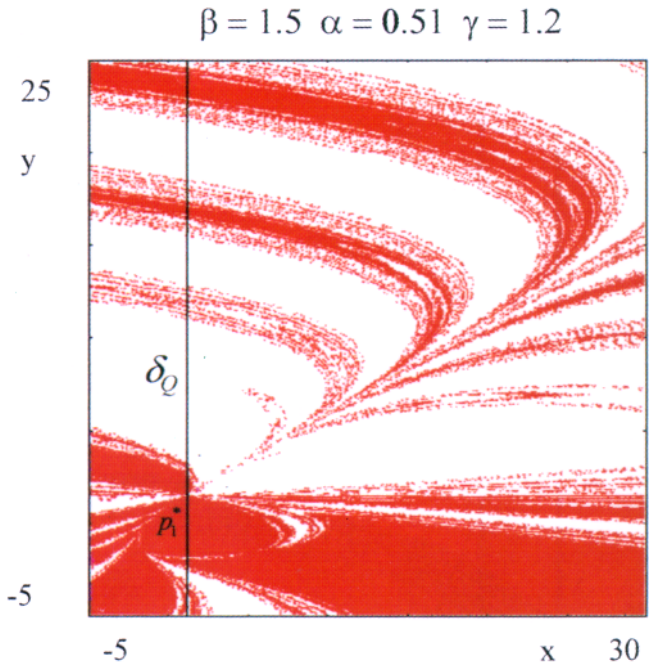

Figure 27.

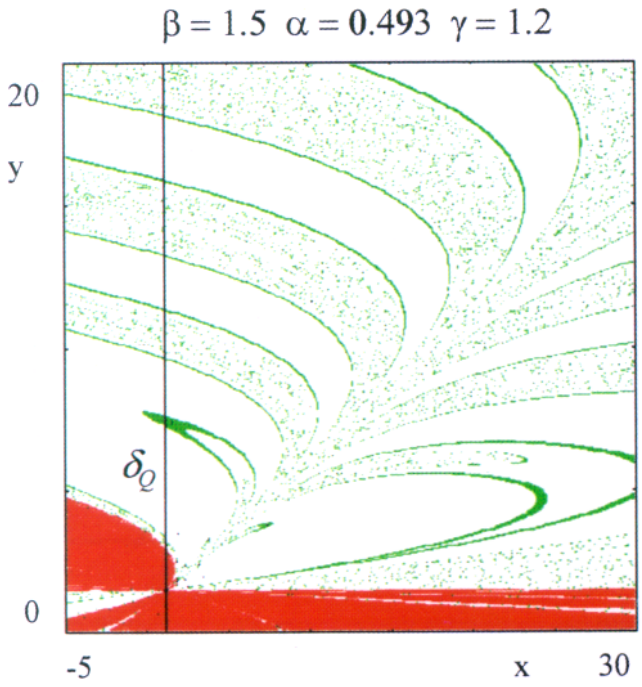

Figure 28.

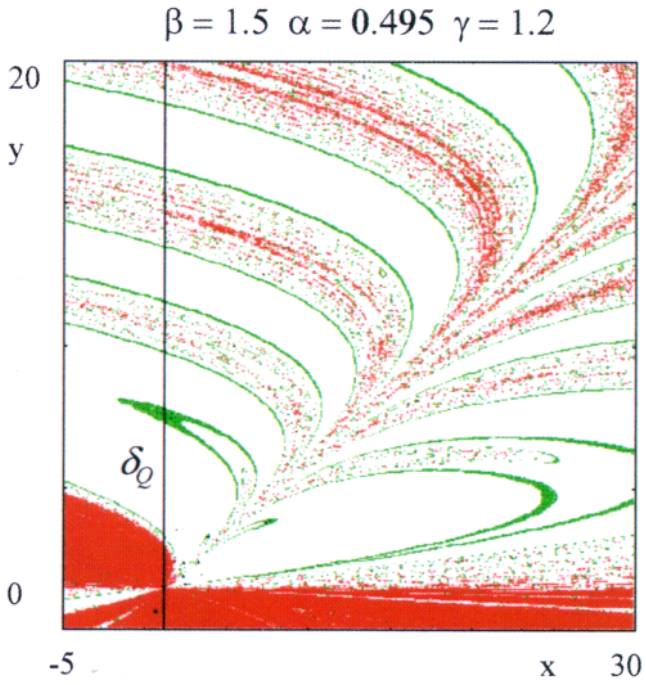

Figure 29.

bounded by δ_s^{-6}, δ_s^{-7}, δ_s^{-8} and δ_s^{-9} are clearly visible. At this stage the narrow tongue of the white basin bounded by δ_s^{-9} has crossed the prefocal line δ_Q, hence δ_s^{-10} (not visible in the figure) bounds a white strip that reaches the focal point Q with a white lobe issuing from it. As the parameter is further increased, more and more white tongues reach the focal points and accumulate below δ_s, thus creating the structure observed in Fig. 25.

For higher values of the parameter α another global bifurcation occurs which causes a sudden explosion of the red basin of the fixed point P_1^* (see Fig. 27, obtained with $\alpha = 0.51$). *Such bifurcation is due to a contact between the unstable manifold*

$W^u(P_2^*)$ *of the saddle* P_2^* *and the singular line* δ_s, occurring at $\alpha = \alpha_h = 0.494\ldots$. Figs. 28 and 29 have been obtained for $\alpha = 0.493$ and $\alpha = 0.495$ respectively, i.e. just before and just after the bifurcation. The red points represent the basin of the stable focus P_1^*, the white points converge to a cycle of period 2 and the green points represent the basin of attraction of a coexisting stable cycle of period 8. The explosion of red points occurring as the parameter α crosses the bifurcation value α_h is rather evident.

The explanation of such a bifurcation can be given by considering the unstable manifold $W^u(P_2^*)$, represented by the black curve in Fig. 30, the stable manifold $W^s(P_2^*)$, represented by the red curve in the same figure, and the line of nondefinition δ_s, represented by the blue curve (in Fig. 30 also its rank-1 preimage δ_s^{-1} is represented by a blue curve).

In Fig. 30(a), obtained for $\alpha < \alpha_h$, $W^u(P_2^*)$ does not intersect the singular line: It is bounded and entirely located above δ_s and on the right of δ_Q. In Fig. 30(b), obtained with $\alpha > \alpha_h$, $W^u(P_2^*)$ intersects the singular line, so that new unbounded branches of $W^u(P_2^*)$ are created that intersect again δ_s and so on. Hence, *just after the bifurcation, infinitely many new* (*and unbounded*) *branches of* $W^u(P_2^*)$ *are created, asymptotic to the line* δ_Q *and to its images as well.*

The points below δ_s, near the intersections with $W^u(P_2^*)$, belong to the basin of P_1^*, and their preimages of any rank, that also belong to $\mathcal{B}(P_1^*)$, after the contact between $W^u(P_2^*)$ and δ_s, are stretched along the stable manifold $W^s(P_2^*)$ and accumulate on it (see the qualitative Fig. 31). In fact, when $W^u(P_2^*)$ has a contact with δ_s in a point A [Fig. 31(b)] then infinitely many preimages δ_s^{-k}, $k = 1, 2, \ldots$, are tangent to $W^u(P_2^*)$, the contact points being the preimages A_{-k} of the point A. The sequence $\{A_{-k}\}$ of preimages of A is convergent, as $k \to \infty$, to P_2^* on the local unstable manifold. All these preimages δ_s^{-k}, $k = 1, 2, \ldots$, bound red tongues of $\mathcal{B}(P_1^*)$ issuing from the focal point, and after the contact these infinitely many tongues cross $W^u(P_2^*)$ and are stretched along $W^s(P_2^*)$, thus giving the explosion of the basin shown in Fig. 29 [see also the qualitative picture in Fig. 31(c)]

Notice that new homoclinic points belonging to $W^u(P_2^*) \cap W^s(P_2^*)$ are created at $\alpha = \alpha_h$ due to the appearance, for $\alpha > \alpha_h$, of the branches of $W^u(P_2^*)$ below the singular line, intersecting the portion of stable set $W^s(P_2^*)$ located below δ_s [see Fig. 30(b)]. Although this homoclinic bifurcation of the saddle P_2^* is not the first one, as homoclinic points of P_2^*, located above δ_s, already exist before this bifurcation, it is of particular type, because it is caused by the creation of a new (unbounded) branch of $W^u(P_2^*)$, due to the contact

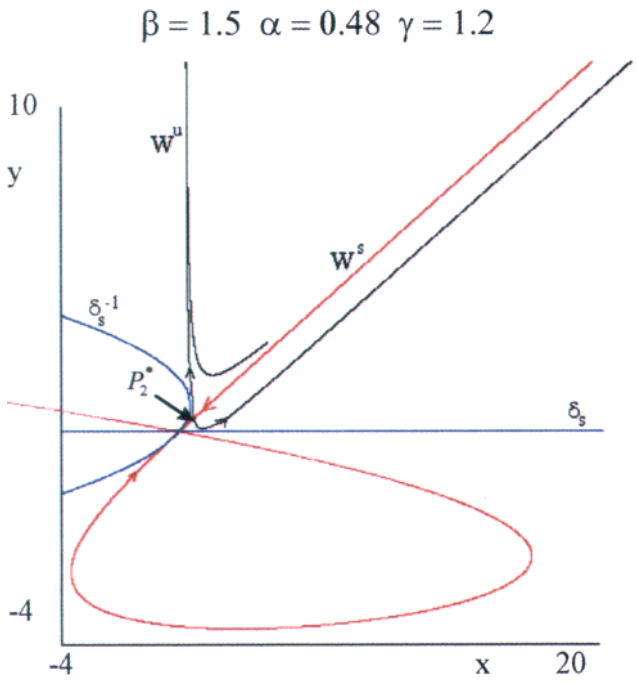

(a)

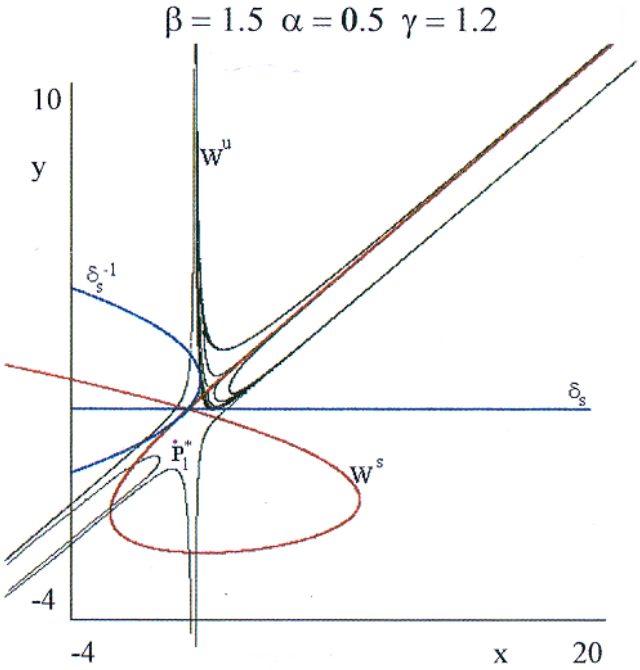

(b)

Figure 30.

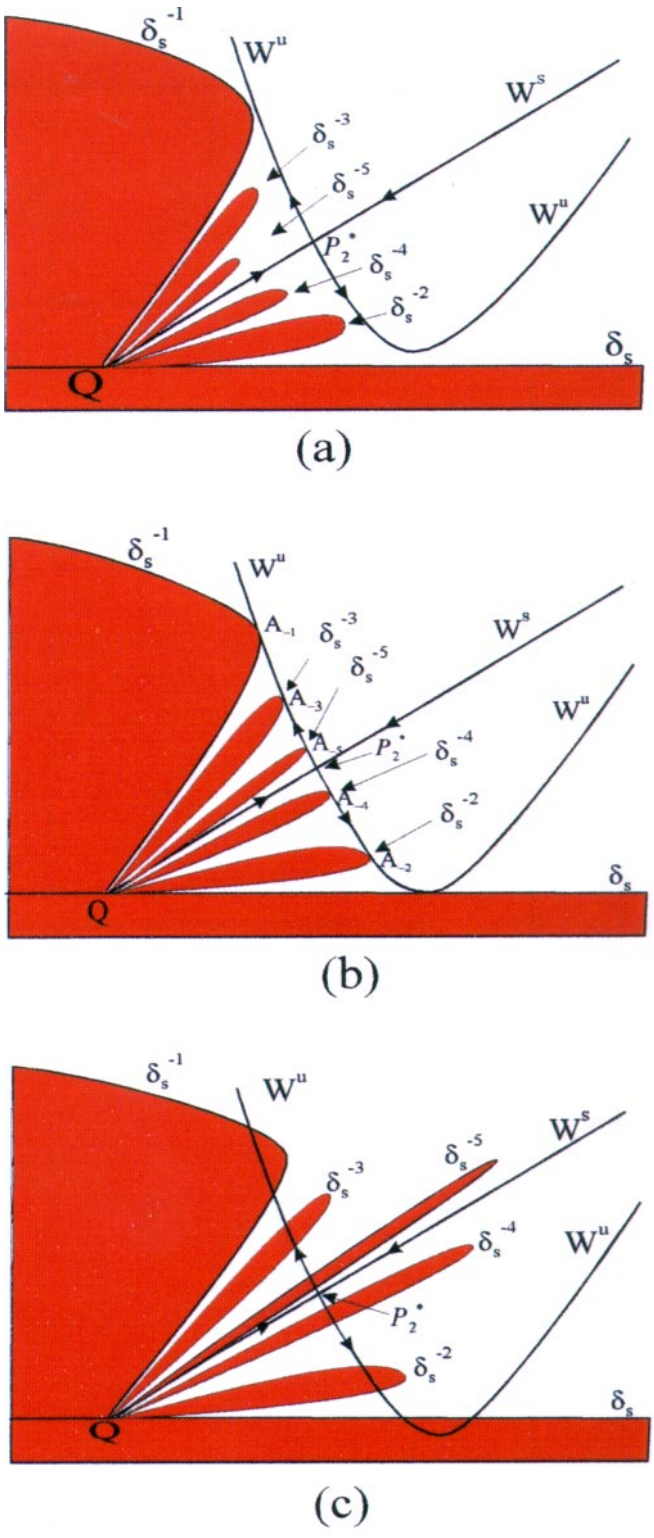

Figure 31.

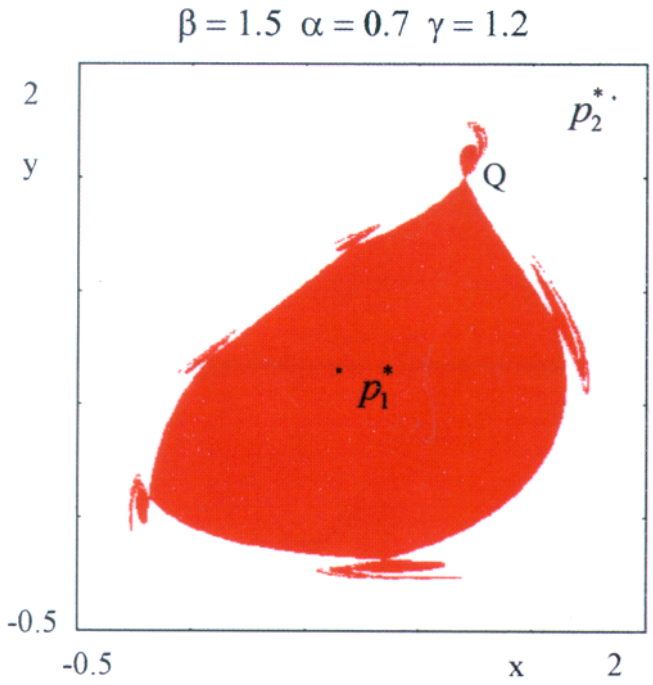

Figure 32.

of $W^u(P_2^*)$ with δ_s. Such new branch, located below δ_s together with its infinitely many preimages, gives rise to infinitely many new intersections between $W^u(P_2^*)$ and $W^s(P_2^*)$, which are not a consequence of a homoclinic tangency between $W^u(P_2^*)$ and $W^s(P_2^*)$, as it usually happens in homoclinic bifurcations of saddles in maps defined in the whole plane.

Another particular structure of the basin of the stable focus P_1^* can be evidenced for higher values of the parameter α, like that shown in Fig. 32, obtained for $\alpha = 0.7$. In order to understand how such basin's structure is created, and which is the role played by the presence of the focal point and the prefocal line, we start from an higher value of α, and then we decrease it. At $\alpha = 0.853\ldots$ a subcritical Neimark–Hopf bifurcation occurs at which the fixed point P_1^* is transformed, for decreasing values of α, from an unstable focus into a stable focus, and a repelling closed invariant curve Γ is created around it which constitutes the basin's boundary, i.e. $\Gamma = \partial\mathcal{B}\,(P_1^*)$ just after the Neimark–Hopf bifurcation (see Fig. 33). As α is decreased the repelling invariant curve Γ enlarges and changes its shape. In particular, since a portion of Γ approaches the prefocal line δ_Q, another portion of it must approach the focal point Q, and when Γ has a contact with the prefocal line the boundary $\partial\mathcal{B}(P_1^*)$ of the basin of P_1^* has a cusp point in Q, and cusp points must exist in all the preimages of Q, that also belong to $\partial B(P_1^*)$ (see Fig. 34). Thus the contact between Γ and δ_Q marks the change from a smooth to a nonsmooth basin boundary. Of course the

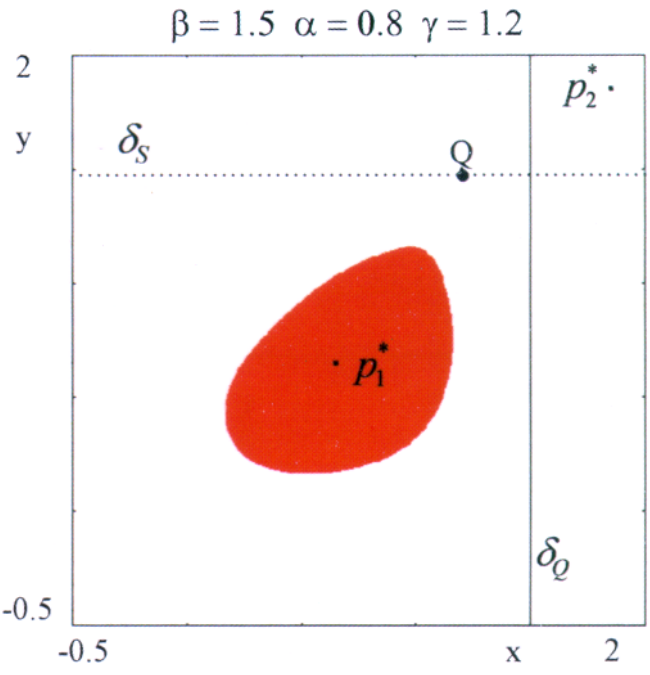

Figure 33.

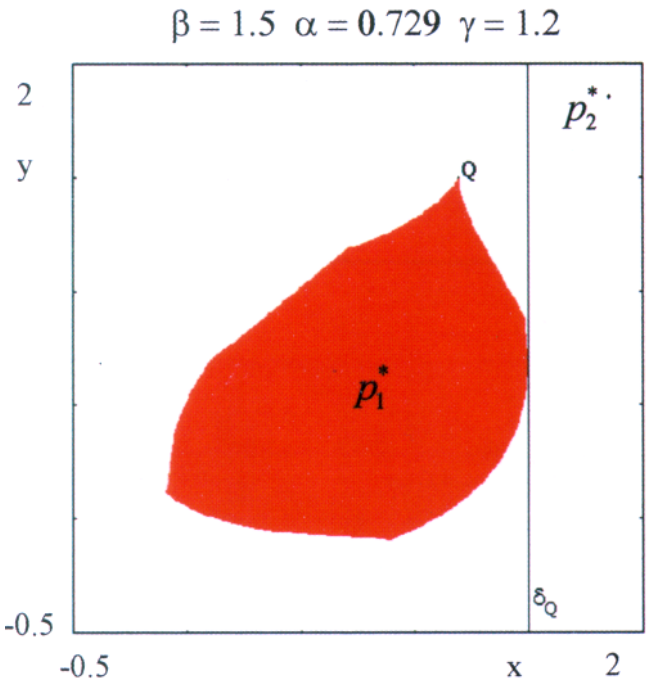

Figure 34.

invariant curve Γ, created at the Neimark–Hopf bifurcation, no longer exists at the bifurcation, since it contains the focal point Q, in which the map is not defined. If α is further decreased a portion of $\partial\mathcal{B}(P_1^*)$ crosses the line δ_Q and lobes are created in Q and its preimages (Fig. 35). This particular bifurcation of a closed invariant set is due

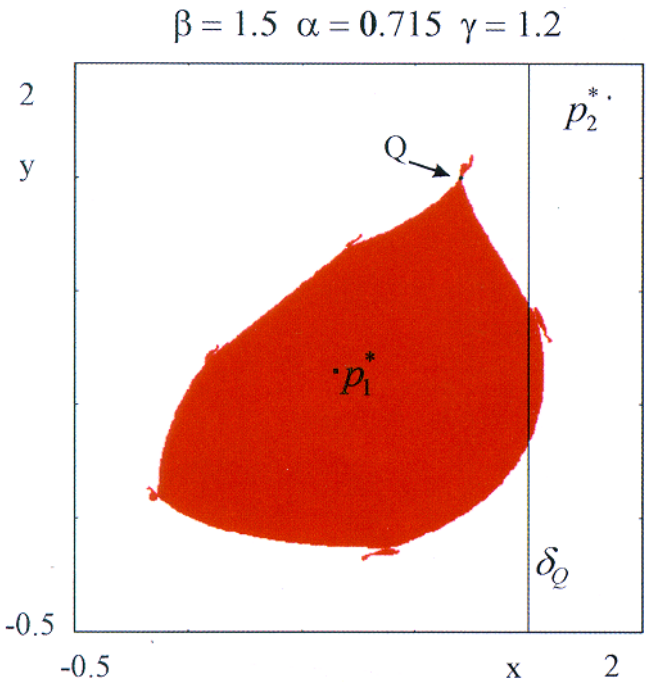

Figure 35.

to a contact with δ_Q: $\partial\overline{B(P_1^*)}$, smooth before the contact, is changed into a nonsmooth set after the contact.

As already remarked in Sec. 2.1, we observe again that even if the map (47) is defined in the whole plane, this does not mean that it is the inverse of (41) in the whole plane. In fact (47) has been obtained from (41) under the assumption $x' \neq \beta$, so that it can be considered as the inverse of (41) only in points out of the line $x' = \beta$. This can also be seen from the fact that the whole line $x' = \beta$ is mapped by (47) into the focal point $Q = (\gamma, \beta)$, i.e. the whole line is "focalized" into the focal point of (41). Of course this implies that (47) is not an invertible map in the whole plane, since the point Q would have infinitely many rank-1 preimages.

3. Polynomial Maps with Fractional Rational Inverses

3.1. *A Polynomial invertible map whose inverse has a focal point*

Consider the map

$$T : \begin{cases} x' = y \\ y' = xy - by^2 - ax + aby \end{cases} \tag{49}$$

with a, b real parameters. This map is defined in the whole plane. Its Jacobian matrix is

$$DT(x, y) = \begin{bmatrix} 0 & 1 \\ y - a & x - 2by + ab \end{bmatrix} \tag{50}$$

hence the Jacobian

$$\det DT(x, y) = y - a \tag{51}$$

vanishes on the line of equation $y = a$. The image of this line is "focalized" by the map T into a single point, being

$$T(\{y = a\}) = (a, 0)\,. \tag{52}$$

From this fact we argue that at least one inverse of (49) must be a map with denominator, and with a focal point in $(a, 0)$ related to a prefocal curve of equation $y = a$.

Indeed, the map (49) can be easily inverted to obtain the fractional map

$$T^{-1} : \begin{cases} x = \dfrac{y + bx'^2 - abx'}{x' - a} \\ y = x' \end{cases} \tag{53}$$

not defined in the line $x' = a$. It is easy to realize that the point $Q = (a, 0)$ is a focal point of T^{-1}, with prefocal line δ_Q of equation $y = a$. In this case the correspondence between slopes of curves through Q and points of δ_Q can be obtained very easily by the second of (14). In fact, from

$$DT(x, a) = \begin{bmatrix} 0 & 1 \\ 0 & x - ab \end{bmatrix} \tag{54}$$

we obtain the correspondence $m \leftrightarrow (x, a)$ with

$$m = x - ab\,. \tag{55}$$

Of course the same result can also be obtained by computing the limit of $T^{-1}(\gamma)$ along an arc γ through Q.[3] Let γ be parameterized as $x' = a + \xi_1\tau + O(\tau^2)$; $y' = \eta_1\tau + O(\tau^2)$. Then

$$\lim_{\tau\to 0} T^{-1}(\gamma(\tau)) = \left(\lim_{\tau\to 0} \frac{\eta_1\tau + ab\xi_1\tau}{\xi_1\tau},\, a\right) = (m + ab,\, a)$$

where $m = \eta_1/\xi_1$, from which $x = m + ab$, as in (55).

These properties of the map (49) and its inverse (53) can have important consequences on the structure of the attractors and their basins of attraction. The map (49) has two fixed points: $O = (0, 0)$ and $P = (a + 1/(1 - b),\, a + 1/(1 - b))$. For the parameter values $a = -0.6$, $b = 0.5$ the fixed point O is an attracting node and $P = (1.4, 1.4)$ is a repelling node. In Fig. 36, obtained with these parameters, the basin of attraction of the stable fixed point O is represented by the white region, whereas the grey region represents the basin of infinity, i.e. the set of points that generate diverging trajectories. Since the point $Q = (0, a)$ is inside the basin of O, also the whole line $y = a$ (the prefocal line of the inverse, which is "focalized" by the map T into the point Q) must belong to the same basin, as well as its preimages of any rank. *This implies that the basin of O cannot be a bounded set because it must necessarily include a whole line and its preimages, which are asymptotes of the basin boundary.*

Another interesting situation is shown in Fig. 37, obtained with $a = -1.5$ and $b = 0.5$. For this set of parameters the fixed point O is a saddle point, and P is a repelling node. A chaotic attractor, that has been created near O through a sequence of period doubling bifurcations, is represented in Fig. 37 together with the basin of bounded trajectories (the white region). The chaotic attractor has a very peculiar shape, characterized by a sort of "knot" of infinitely many curves that shrink into a unique point, the point $Q = (0, a)$, which is the focal point of the inverse map (53). In fact, every trajectory contained inside the attractor is conveyed through Q whenever it crosses the line $y = a$. In particular, Q is the centre of a fan of unstable sets of saddle cycles belonging to the chaotic area, such as the fixed point O, or of unstable sets of cycles belonging to the basin boundary.

However, the "structure" of such an attracting set must be more complex of what we see at a first glance because all the images of the knot-point, that belong to the attracting set, behave in the same way.

[3] We do not apply directly (12) or (13) because the map (49) is not in the form (3). However the procedure followed to obtain (12) can be easily repeated with obvious changes.

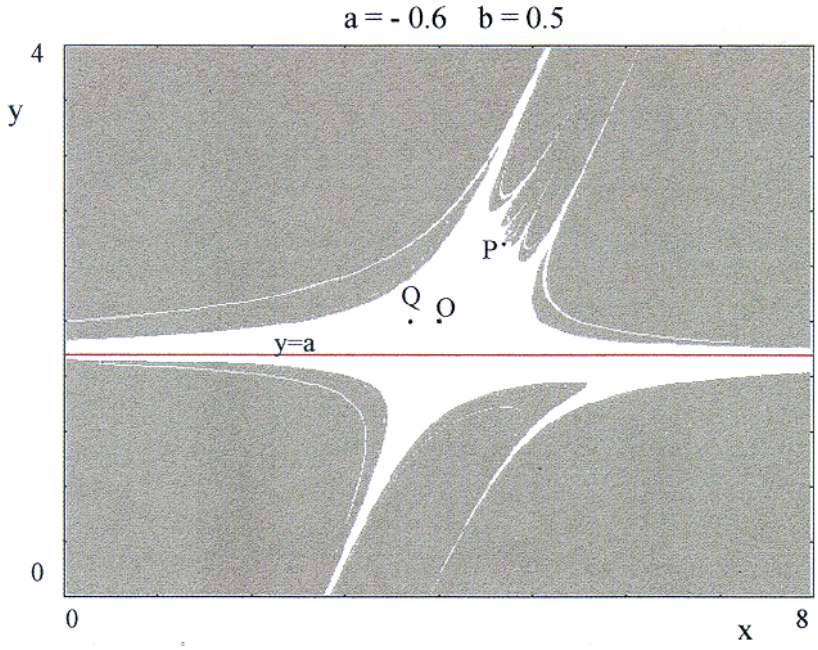

Figure 36.

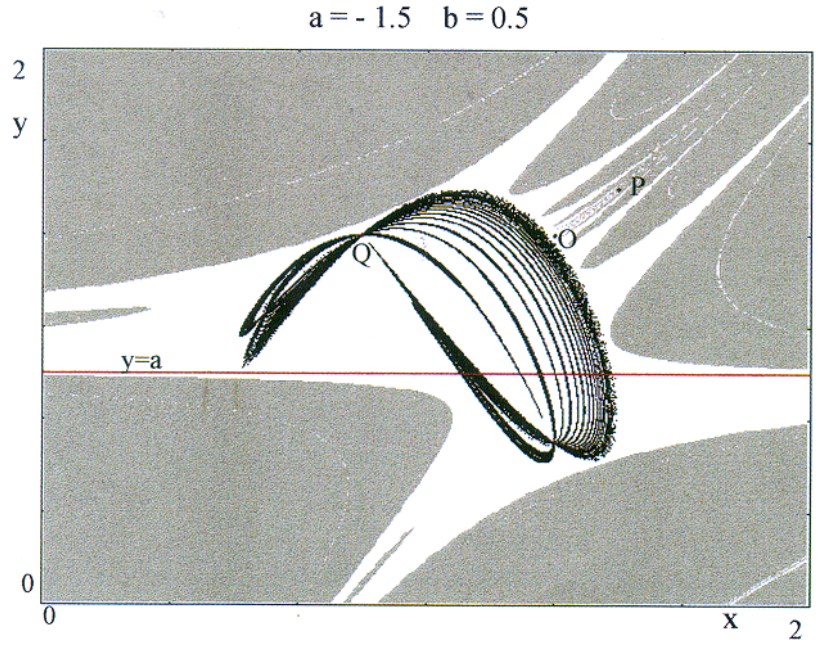

Figure 37.

3.2. *A Triangular noninvertible map of $Z_0-Z_2-Z_4$ type, whose inverses have a focal point*

Consider the map [Mira *et al.*, 1996, p. 226]

$$T: \begin{cases} x' = x^2 - a \\ y' = bxy(1-y) \end{cases} \tag{56}$$

with a, b real parameters. Also this map is defined in the whole plane, and its Jacobian matrix is

$$DT(x, y) = \begin{bmatrix} 2x & 0 \\ by(1-y) & bx(1-2y) \end{bmatrix}. \tag{57}$$

Its Jacobian determinant

$$\det DT(x, y) = 2bx^2(1-2y) \tag{58}$$

vanishes on the lines of equation $y = 1/2$ and $x = 0$. The image of the line $y = 1/2$ is given by the parabola of equation

$$x = \frac{16}{b^2} y^2 - a \tag{59}$$

whereas the whole y axis is mapped by T into one point, being

$$T(\{x = 0\}) = (-a,\, 0)\,. \tag{60}$$

As in the previous example, we argue that at least one inverse of (56) must exist which is a fractional map with a focal point in $(-a,\, 0)$ and prefocal curve on the y axis. However in this case we do not expect that the map T has a unique inverse, since the curve (59) is a critical curve LC, locus of merging preimages, that separates regions characterized by a different number of inverses. In fact the map T has up to four distinct inverses, given by

$$T_1^{-1} : \begin{cases} x = \sqrt{x' + a} \\ y = \dfrac{1}{2}\left(1 + \sqrt{1 - \dfrac{4y'}{b\sqrt{x' + a}}}\right) \end{cases};$$

$$T_2^{-1} : \begin{cases} x = \sqrt{x' + a} \\ y = \dfrac{1}{2}\left(1 - \sqrt{1 - \dfrac{4y'}{b\sqrt{x' + a}}}\right) \end{cases}$$

defined for $x' > -a$ and $y \le b/4\sqrt{x' + a}$, and

$$T_3^{-1} : \begin{cases} x = -\sqrt{x + a} \\ y = \dfrac{1}{2}\left(1 + \sqrt{1 + \dfrac{4y}{b\sqrt{x + a}}}\right) \end{cases};$$

$$T_4^{-1} : \begin{cases} x = -\sqrt{x + a} \\ y = \dfrac{1}{2}\left(1 - \sqrt{1 + \dfrac{4y}{b\sqrt{x + a}}}\right) \end{cases}$$

defined for $x' > -a$ and $y \ge -b/4\sqrt{x' + a}$.

From the expressions of the inverses we can see that not only the critical curve LC defined in (59) separates regions whose points have different number of preimages, but also the vertical line of equation $x = -a$. In fact, the plane $(x,\, y)$ can be divided into four regions (see Fig. 38):

1. $Z_0 = \{(x,\, y) | x < -a\}$ whose points have no preimages, i.e. no inverses are defined in this region;

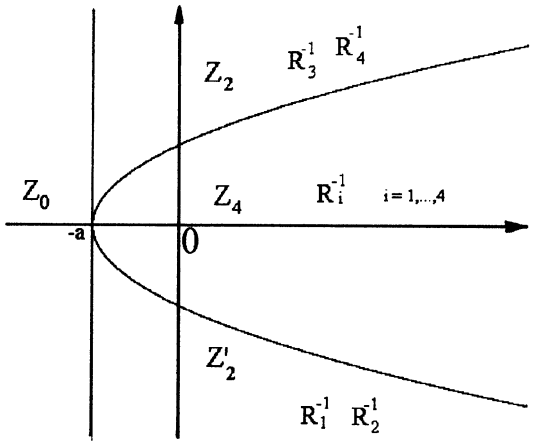

Figure 38.

2. $Z_2 = \{(x,\, y) | x > -a$ and $y \ge b/4\sqrt{x - a}\}$ where the inverses T_3^{-1} and T_4^{-1} are defined;
3. $Z_2' = \{(x,\, y) | x > -a$ and $y \le -b/4\sqrt{x - a}\}$ where the inverses T_1^{-1} and T_2^{-1} are defined;
4. $Z_4 = \{(x,\, y) | x > -a$ and $-b/4\sqrt{x - a} \le y \le b/4\sqrt{x - a}\}$ where the four inverses are defined.

It can be noticed that the line $x = -a$ separates regions with different numbers of inverses, but it is not a critical curve. The only peculiarity of that line lies in the fact that it is the curve at which the denominator of the inverses vanishes.

Roughly speaking, we can say that for the map (56) the line $x = -a$ plays a role analogue to that of a horizontal asymptote in a one-dimensional map. In fact, as it is well known, a horizontal asymptote can separate, in the range of a one-dimensional map, regions characterized by a different number of inverses. As an example, consider the map

$$x' = f(x) = \frac{1}{1 + x^2} \tag{61}$$

whose graph is shown in Fig. 39(a). The critical point $c = f(0) = 1$ separates the regions Z_2 and Z_0 where two and no inverses are defined respectively, and the horizontal asymptote $y = 0$ separates the regions Z_2 and Z_0'. Of course a horizontal asymptote of a map corresponds to a vertical asymptote for at least one of its inverses. For example, both the inverses of the map (61), given by

$$f_1^{-1} = \sqrt{\frac{1 - x'}{x'}} \qquad \text{and} \qquad f_2^{-1} = -\sqrt{\frac{1 - x'}{x'}}$$

have a vertical asymptote of equation $x' = 0$ [see Figs. 39(b) and 39(c)].

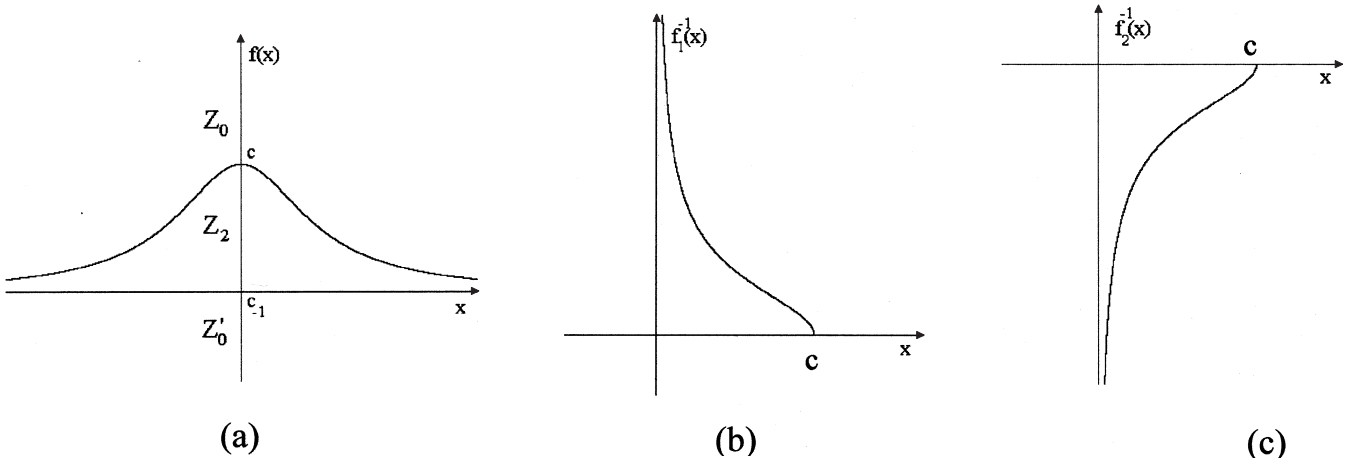

Figure 39.

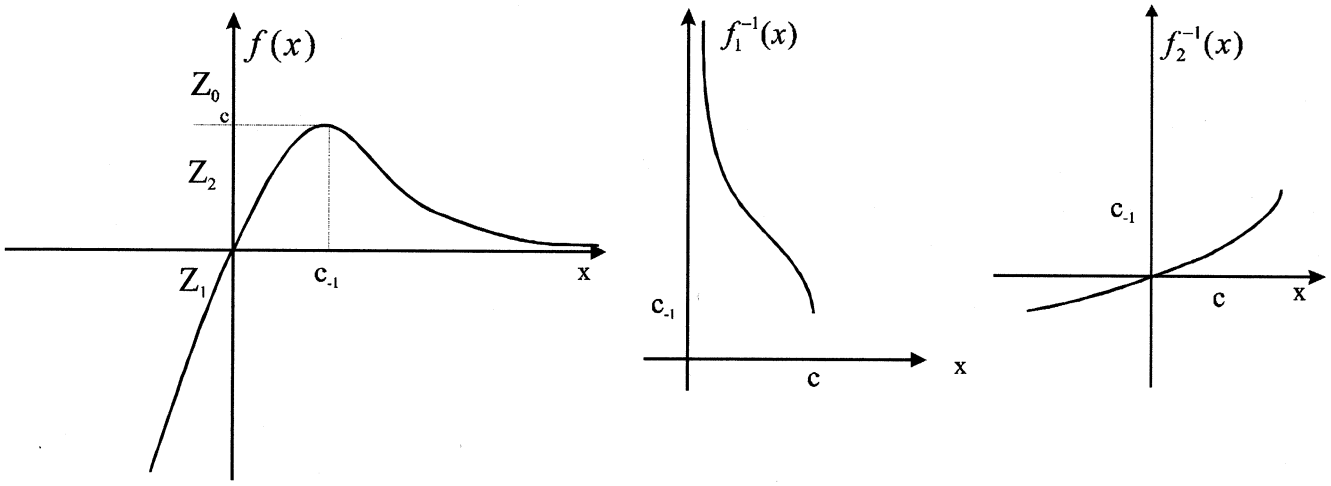

Figure 40.

Many other examples of one-dimensional maps, in which the horizontal asymptotes separate the real axis into regions whose points have different number of preimages, can be given. For example, the graph of Fig. 40 represents a one-dimensional map in which the horizontal asymptote separates the real axis into the regions Z_2 and Z_1, where two and one inverses are defined respectively. It can also be noticed that in this case the horizontal asymptote becomes a vertical asymptote for only one of the two inverse maps.

These one-dimensional examples suggest us an heuristic "geometrical" interpretation of the set of points at which a denominator vanishes which are not focal. In fact, roughly speaking, these points can be considered, for a two-dimensional map T, as the two-dimensional analogue of a vertical asymptote. Following the same analogy, the set δ_s of an inverse of T (except for the focal points) plays the role of a vertical asymptote of T^{-1} and, at the same time, of an "horizontal asymptote" for the map T.

As in the one-dimensional case, also for a two-dimensional map an "horizontal asymptote" may separate regions having a different number of rank-1 preimages, and the difference in the number of preimages between such regions is not necessarily a multiple of 2 (as it occurs for critical curves). For example, for a two-dimensional map, the presence of a curve which belongs to the set of points in which a denominator of at least one inverse map vanishes, can be a curve that separates a region Z_k from a region Z_{k+2}, or Z_k from Z_{k+1}, or even Z_k from Z'_k, where Z_k and Z'_k indicate two regions whose points have the same number k of rank-1 preimages, but obtained by different inverses, as we shall see in the next examples.

3.2.1. *A noninvertible $Z_0 - Z_2$ map whose inverses have a "vertical asymptote"*

Consider the map

$$T : \begin{cases} x' = ax(1-x) - axy \\ y' = bxy \end{cases} \tag{62}$$

proposed in [Cathala & Barugola, 1996] (see also [Mira *et al.*, 1996, p. 197]. From the Jacobian matrix

$$DT(x, y) = \begin{bmatrix} a - 2ax - ay & -ax \\ by & bx \end{bmatrix} \tag{63}$$

we see that the Jacobian

$$\det(DT) = abx(1-2x) \tag{64}$$

vanishes on the two lines of equation $x = 0$ and $x = 1/2$. The former is "focalized" by the map T into a single point, since $T(\{x = 0\}) = (0, 0)$. Thus we expect that the map T has at least one inverse with denominator, and such that $Q = (0, 0)$ is a focal point with the y axis as corresponding prefocal line δ_Q. In fact the inverses

$$T_1^{-1} : \begin{cases} x = \dfrac{1}{2}\left(1 + \sqrt{1 - 4\left(\dfrac{x'}{a} + \dfrac{y'}{b}\right)}\right) \\ y = \dfrac{2y'}{b\left(1 + \sqrt{1 - 4\left(\dfrac{x'}{a} + \dfrac{y'}{b}\right)}\right)} \end{cases};$$

$$T_2^{-1} : \begin{cases} x = \dfrac{1}{2}\left(1 - \sqrt{1 - 4\left(\dfrac{x'}{a} + \dfrac{y'}{b}\right)}\right) \\ y = \dfrac{2y'}{b\left(1 - \sqrt{1 - 4\left(\dfrac{x'}{a} + \dfrac{y'}{b}\right)}\right)} \end{cases} \tag{65}$$

are such that one of them, T_2^{-1}, has a focal point in $Q = (0, 0)$ with the y axis as prefocal line. The relation between slopes of arcs through Q and the points of δ_Q can be easily obtained from (14) applied to $DT(0, y)$:

$$m = \frac{by}{a(1-y)}\,. \tag{66}$$

The other line on which the Jacobian vanishes, $x = 1/2$, is a curve of merging preimages, LC_{-1}. In fact, its image by T is the line of equation

$$\frac{x}{a} + \frac{y}{b} = \frac{1}{4} \tag{67}$$

which is a critical curve, $LC = T(LC_{-1})$, locus of points with two merging preimages, that separates the plane into the two regions Z_2 and Z_0 where two and no inverses are defined respectively. However in [Cathala & Barugola, 1996] it is stressed that for the points of the line Γ, of equation $bx' + ay' = 0$, only one inverse, T_1^{-1}, is defined, since the denominator of T_2^{-1} vanishes on the points of the line Γ, so that Γ separates the region Z_2 into two regions, denoted by Z_2' and Z_2'' in [Cathala & Barugola, 1996] [see also Fig. 41(b)].

Also in this case we can say, following the analogy discussed above, that the line Γ behaves as a vertical asymptote for one of the inverses, and constitutes the two-dimensional analogue of a horizontal asymptote for the map (62). A one-dimensional map showing a property similar to that of the map T can be easily found. Consider, for example, the map

$$x' = \frac{x^2}{(1+x)^2} \tag{68}$$

whose graph is shown in Fig. 41(a). The horizontal asymptote $x' = 1$ separates two regions, say Z_2' and Z_2'', both with points that have two rank-1 preimages, but obtained by different inverses. For $x' = 1$ only one preimage exists, given by $x = -1/2$, while a critical point, $x' = 0$, separates the regions Z_2'' and Z_0.

4. Some Definitions and Properties of Maps Defined by an Implicit Form

In the previous section we have suggested a geometrical interpretation, based on analogies with one-dimensional maps, of the non-focal points of the set δ_s at which a denominator of a map T of the plane vanishes, but we have not discussed any possible one-dimensional analogue for a focal point and its associated prefocal set. Indeed it is not easy to imagine something similar in one-dimensional maps. A possibility is that of considering a graph like that shown in Fig. 42. Clearly this is not the graph of a function $x' = f(x)$, because in the point $x = Q$ it is not single-valued. If we are allowed to write $f(Q) = [\alpha, \beta]$ then Q behaves

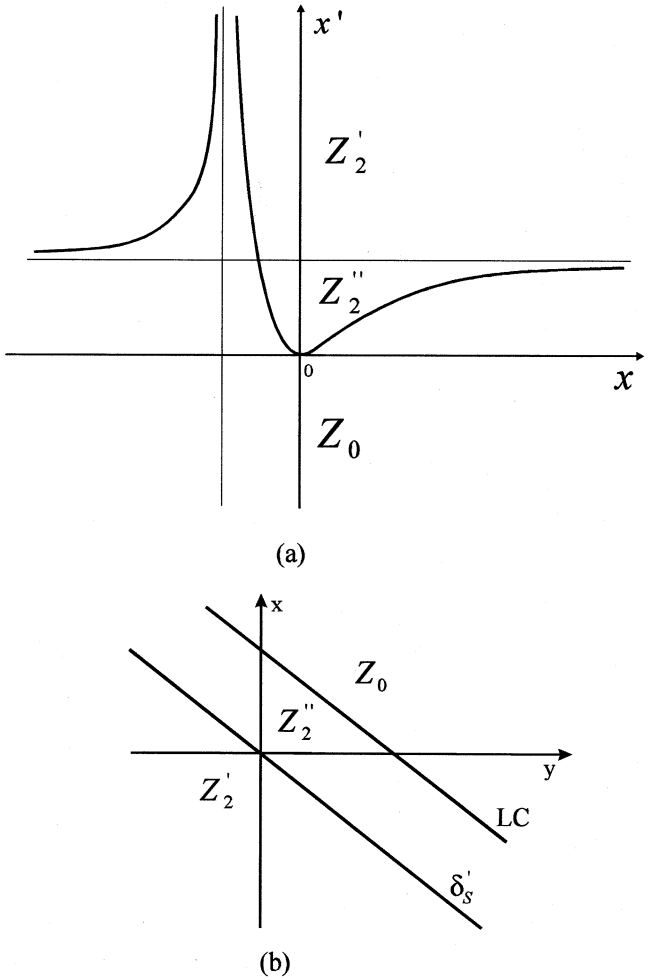

Figure 41.

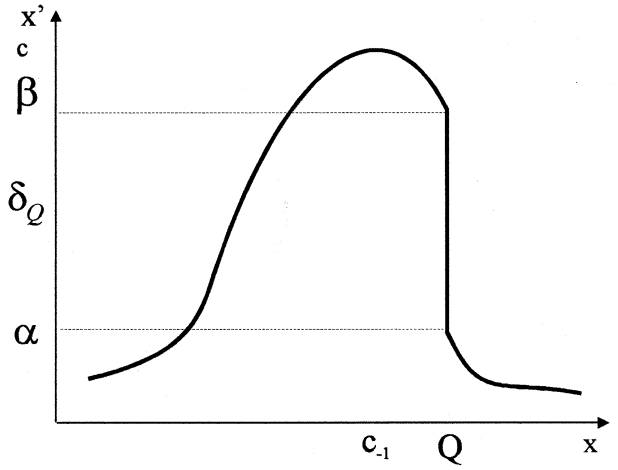

Figure 42.

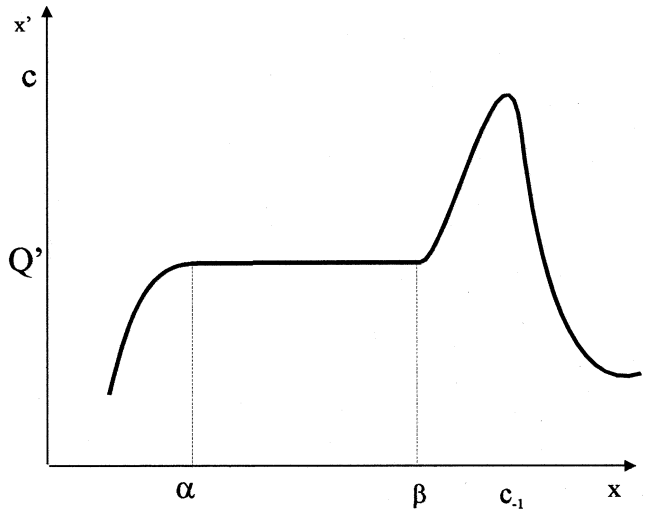

Figure 43.

as a one-dimensional "focal point", whose associated prefocal set δ_Q is the segment $[\alpha, \beta]$. The two inverse functions f_a^{-1} and f_b^{-1}, defined for $x' < c$ and taking values on the left and on the right of the critical point $x = c_{-1}$ respectively, are single valued. Using the same notations introduced in the previous sections we have $f_b^{-1}([\alpha, \beta]) = Q$ and $d/dx' f_b^{-1}(x') = 0 \ \forall x' \in [\alpha, \beta]$.

In order to draw an analogy with the class of maps analyzed in Sec. 3, we consider the function $x' = f(x)$ with a graph like that shown in Fig. 43. In this case $f(x)$ is a single-valued function, but this is not true for all its inverses. In fact, let f_a^{-1} be the inverse of f that takes values in the range $x < c_{-1}$. Indeed, the map $f(x)$ is not invertible in $[\alpha, \beta]$ since $f'(x) = 0$ for each $x \in [\alpha, \beta]$. However, using the notations of the previous sections, we can say that $f[\alpha, \beta] = Q'$, thus f_a^{-1} is not a single valued function because we ought to write $f_a^{-1}(Q') = [\alpha, \beta]$. Also in this case we can say that the point Q' is a one-dimensional analogue of a focal point of the inverse f_a^{-1} and $\delta_{Q'} = [\alpha, \beta]$ is the related prefocal set.

A method for the description of both the situations represented in Figs. 42 and 43 can be obtained by the definition of an implicit equation in the form

$$h(x, x') = 0 \tag{69}$$

from which both the relations $x' = f(x)$ and $x = f^{-1}(x')$ can be obtained. In the following we assume that at least one of the two explicit forms obtained from (69) is singled valued. The graph of the relation (69) is, as usual, the set of points (x, x') for which (69) holds true. In particular, the implicit relation (69) is satisfied by the sets $\{(Q, x') | \, x' \in \delta_Q\}$ or $\{(x, Q') | \, x \in \delta_{Q'}\}$ in the situations represented in Figs. 42 and 43 respectively.

In these cases we can write, more synthetically, $h(Q, \delta_Q) = 0$ or $h(\delta_{Q'}, Q') = 0$ respectively.

The implicit representation of a one-dimensional map given in (69) is often met in applications, and the presence of denominators is often the result of the necessity of writing an explicit map of the form $x' = f(x)$. A sufficient condition to obtain a single valued explicit function is provided by the implicit function theorem: if $\partial h/\partial x(\overline{x}, \overline{x}') \neq 0$ then the single-valued function $x' = f(x)$ can be obtained, defined at least in a neighborhood of $\overline{x}$. Thus the condition $\partial h/\partial x'(Q, x') = 0 \, \forall x' \in \delta_Q$ is a necessary condition for a focal point Q, with prefocal set δ_Q, as in the situation shown in Fig. 42.

A similar reasoning can be followed for the case of maps of the plane, where the implicit relation (69) is substituted by the following equations

$$\begin{cases} H_1(x, y, x', y') = 0 \\ H_2(x, y, x', y') = 0 \end{cases}$$

or, in a more compact vector notation

$$\mathbf{H}(x, y, x', y') = 0 \tag{70}$$

whose graph is a two-dimensional subset of $\Re^4$. In the following we assume that (70) is of class $C^{(1)}$ in the whole space $\Re^4$. From (70) the explicit relations $(x', y') = T(x, y)$ and $(x, y) = T^{-1}(x', y')$, between the points of the planes (x, y) and (x', y'), can be obtained, not necessarily defined in the whole plane. *We assume that at least one of the explicit relations T or T^{-1} is single valued.*

The existence, for the explicit form T, of a focal point Q with related prefocal set δ_Q, is defined by the identity

$$\mathbf{H}(Q, x', y') = 0 \quad \forall (x', y') \in \delta_Q \tag{71}$$

or, more synthetically, $\mathbf{H}(Q, \delta_Q) = 0$. Analogously, the presence of a focal point Q for the explicit form T^{-1}, with associated prefocal set $\delta_{Q'}$, is defined by the identity

$$\mathbf{H}(x, y, Q') = 0 \quad \forall (x, y) \in \delta_{Q'} \tag{72}$$

or, more synthetically, $\mathbf{H}(\delta_{Q'}, Q') = 0$.

From the Jacobian matrix

$$\frac{\partial \mathbf{H}}{\partial(x, y, x', y')} = \begin{bmatrix} \dfrac{\partial H_1}{\partial x} & \dfrac{\partial H_1}{\partial y} & \dfrac{\partial H_1}{\partial x'} & \dfrac{\partial H_1}{\partial y'} \\ \dfrac{\partial H_2}{\partial x} & \dfrac{\partial H_2}{\partial y} & \dfrac{\partial H_2}{\partial x'} & \dfrac{\partial H_2}{\partial y'} \end{bmatrix} \tag{73}$$

the Jacobians of T and T^{-1} can be easily computed, being

$$\begin{aligned} \det[DT(x, y)] &= \frac{\det\left[\dfrac{\partial \mathbf{H}}{\partial(x, y)}\right]}{\det\left[\dfrac{\partial \mathbf{H}}{\partial(x', y')}\right]}; \\ \det[DT^{-1}(x', y')] &= \frac{\det\left[\dfrac{\partial \mathbf{H}}{\partial(x', y')}\right]}{\det\left[\dfrac{\partial \mathbf{H}}{\partial(x, y)}\right]} \end{aligned} \tag{74}$$

the first one expressed with the variables x and y, using, if necessary, the explicit relation $(x', y') = T(x, y)$, the second one expressed with the variables x' and y', using, if necessary, the explicit relation $(x, y) = T^{-1}(x', y')$.

This suggests a method to find the focal points and prefocal sets for T or T^{-1} starting from the implicit relation (70). Let $J_0^{'}$ be the locus of points at which the Jacobian of T^{-1} vanishes, i.e.

$$J_0^{'} = \{(x', y') | \det(DT^{-1}(x', y')) = 0\}. \tag{75}$$

A point Q is a focal point of T, with associated prefocal curve δ_Q, if

$$\delta_Q \in J_0^{'} \qquad \text{and} \qquad \mathbf{H}(Q, \delta_Q) = 0. \tag{76}$$

A similar method can be used to find the focal points and prefocal sets of T^{-1}: let J_0 be the locus of points at which the Jacobian of T vanishes, i.e.

$$J_0 = \{(x, y) | \det(DT(x, y)) = 0\}. \tag{77}$$

A point Q is a focal point of T^{-1}, with associated prefocal curve $\delta_{Q'}$, if

$$\delta_{Q'} \in J_0 \qquad \text{and} \qquad \mathbf{H}(\delta_{Q'}, Q') = 0. \tag{78}$$

This method can be easily applied to find the focal points and the prefocal sets of the maps we have considered in the previous sections. Consider, for example, the map (17). It can be obtained from the implicit relation:

$$\begin{cases} y - x' = 0 \\ yy' - \beta y' - y^2 + \lambda xy \\ \qquad + \beta y - \beta\lambda x - \alpha x^2 - \gamma x = 0 \end{cases} \tag{79}$$

defined for each $(x, y, x', y') \in \Re^4$.

From (79) the explicit relations T and T^{-1} can be obtained: the relation T is the single valued map (17), defined for $y \neq \beta$, and the inverse relation T^{-1} is given by $T^{-1} = T_1^{-1} \cup T_2^{-1}$, where T_1^{-1} and T_2^{-1} are given in (22). We now show how the prefocal sets and focal points can be found through

the study of the Jacobian matrix of the implicit relation (79):

$$\frac{\partial H}{\partial(x,\, y,\, x',\, y')} = \begin{bmatrix} 0 & 1 & -1 & 0 \\ \lambda y - 2\alpha x - \beta\lambda - \gamma & y' - 2y + \lambda x + \beta & 0 & y - \beta \end{bmatrix}$$

from which

$$\det[DT(x,\, y)] = \frac{\det\left[\dfrac{\partial H}{\partial(x,\, y)}\right]}{\det\left[\dfrac{\partial H}{\partial(x',\, y')}\right]} = \frac{-\lambda y + 2\alpha x + \beta\lambda + \gamma}{\beta - y}\,,$$

$$\det[DT_1^{-1}(x',\, y')] = \frac{\det\left[\dfrac{\partial H}{\partial(x',\, y')}\right]}{\det\left[\dfrac{\partial H}{\partial(x,\, y)}\right]} = \frac{\beta - x'}{-\lambda x + 2\alpha x_1(x',\, y') + \beta\lambda + \gamma}$$

and

$$\det[DT_2^{-1}(x',\, y')] = \frac{\det\left[\dfrac{\partial H}{\partial(x',\, y')}\right]}{\det\left[\dfrac{\partial H}{\partial(x,\, y)}\right]} = \frac{\beta - x'}{-\lambda x + 2\alpha x_2(x',\, y') + \beta\lambda + \gamma}$$

where $x_1(x',\, y')$ and $x_2(x',\, y')$ represent, respectively, the first component of T_1^{-1} and T_2^{-1} given in (22). From the condition $\det(DT(x,\, y)) = 0$ we obtain the equation

$$\lambda y - 2\alpha x + \gamma - \beta\lambda - \gamma = 0\,,$$

which defines the set LC_{-1} of merging preimages given in (26), whose image by T is the critical curve LC of Eq. (21). Instead, from the condition $\det(DT^{-1}(x',\, y')) = 0$ we obtain the line δ_Q of equation $x' = \beta$, whose images by T_1^{-1} and T_2^{-1} can be easily obtained through the implicit relation (83). In fact, with $x' = \beta$ (79) becomes

$$\begin{cases} y = \beta \\ -\alpha x^2 - \gamma x = 0 \end{cases}$$

from which the points $Q^1 = (-\gamma/\alpha,\, \beta)$ and $Q^2 = (0,\, \beta)$ are obtained. This is equivalent to say that $T_1^{-1}(\{x' = \beta\}) = Q^1$ and $T_2^{-1}(\{x' = \beta\}) = Q^2$, which means that Q^1 and Q^2 are two focal points associated with the same prefocal line δ_Q of equation $y = \beta$.

The application of this method to the other examples proposed in this paper, in order to find the focal points and prefocal sets of the maps, and of their inverses, is a simple exercise which is left to the reader.

5. Conclusions

In this paper we have studied some global dynamical properties and bifurcations of two-dimensional maps, related to the presence, in the map or in one of its inverses, of a vanishing denominator. Some new kinds of contact bifurcations have been evidenced, whose description can be made through the definition of new concepts, specific of maps with vanishing denominator, like the *set of non-definition*, the *focal points* and the *prefocal curves*. These concepts allowed us to give a geometric characterization to some new bifurcations which change the structure of the basin boundaries, and to describe a new mechanism for the occurrence of homoclinic bifurcations specific to maps with vanishing denominator.

We have shown, through theoretical arguments and examples, that these concepts are also useful to understand some particular properties observed in maps defined in the whole plane (for example polynomial maps) related to the presence of a vanishing denominator in at least one inverse map. In particular, for noninvertible maps, we have shown that the locus of points in which the denominator of some inverse vanishes may separate regions of the phase plane whose points have a different number of preimages. Such points are the two-dimensional analogue of a horizontal asymptote of a one-dimensional map (which corresponds to a vertical asymptote of at least one inverse) which separates zones with different numbers of preimages.

The presence of inverse maps with vanishing denominator imply that the locus of points J_0 at which the Jacobian of a map vanishes may include a whole curve which is entirely mapped into a single point, a property often observed in maps studied in the literature. We have shown that these particular curves, whose properties are different from those of the critical points even if they belong to J_0, may have a strong influence on the dynamical properties of the map, and are related to the presence of a prefocal curve of one inverse map.

Other important bifurcations (for example due to the merging of focal points, or to the merging of focal points and fixed points, or to contacts between prefocal curves and critical curves) have not been considered in the present paper, and will be the object of further studies.

Acknowledgments

The work has been performed under the activity of the research project "Dinamiche nonlineari ed applicazioni alle scienze economiche e sociali", MURST, Italy, the financial support of CNR, Italy, and under the auspices of GNFM, CNR, Italy.

References

Abraham, R., Gardini, L. & Mira, C. [1997] *Chaos in Discrete Dynamical Systems, A Visual Introduction in Two-Dimension*, (Springer-Verlag).

Barucci, E., Bischi, G. I. & Marimon, R. [1998] "The stability of inflation target policies," *mimeo* (European University Institute, Florence), 1–40.

Billings, L. & Curry, J. H. [1996] "On noninvertible maps of the plane: Eruptions," *Chaos* **6**, 108–119.

Billings, L., Curry, J. H. & Phipps, E. [1997] "Lyapunov exponents, singularities, and a riddling bifurcation," *Phys. Rev. Lett.* **79**(6), 1018–1021.

Bischi, G. I. & Gardini, L. [1997] "Basin fractalization due to focal points in a class of triangular maps," *Int. J. Bifurcation and Chaos* **7**(7), 1555–1577.

Bischi, G. I. & Gardini, L. [1996] "Focal points and basin fractalization in some rational maps," *Proc. ECIT96 Urbino, Italy, Sept. 96*, in "Grazer Mathematische Berichte", to appear.

Bischi, G. I. & Naimzada, A. [1997] "Global analysis of a nonlinear model with learning," *Econ. Notes* **26**(3), 143–174.

Bischi, G. I. & Naimzada, A. [1995] "A coweb model with learning effects," *Atti XIX Convegno AMASES*, pp. 162–177 (Cacucci Editore, Bari).

Brock, W. A. & Hommes, C. H. [1997] "A rational route to randomness," *Econometrica* **65**(5), 1059–1095.

Cathala, J. C. & Barugola, A. "On the basin boundary of a quadratic degenerate two-dimensional endomorphism," *Proc. ECIT96 Urbino, Italy, Sept. 96, European Conf. Iteration Theory*, in "Grazer Mathematische Berichte", to appear.

Gardini, L. & Bischi, G. I. [1996] "Focal points and focal values in rational maps," *Proc. ECIT96 Urbino, Italy, Sept. 96, European Conf. Iteration Theory*, in "Grazer Mathematische Berichte", pp. 225–231.

Gumowski, I. & Mira, C. [1980] *Dynamique Chaotique* (Cepadues Editions, Toulouse).

Gumowski, I. & Mira, C. [1978] "Bifurcation déstabilisant une solution chaotique d'un endomorphisme du 2nd ordre," *Comptes Rendus Acad. Sci. Paris, Série A* **286**, pp. 427–431.

Julia, G. [1929] "Remarques sur les transformations ponctuelles planes au visinage d'un point ou le jacobien est nul," *Bull. des Sciences methém. 2 series*, t. LIII.

Grebogi, C., Ott, E. & Jork, J. A. [1983] "Crises, sudden changes in chaotic attractors and transient chaos," *Physica* **D7**, 181–200.

Marimon, R. & Sunder, S. [1994] "Expectations and learning under alternative monetary regimes: An experimental approach," *Econ. Theory* **4**, 131–162.

Mira, C. [1981] "Singularités nonclassiques d'une récurrence et d'une équation différentielle d'ordre deux," *Comptes Rendus Acad. Sc. Paris, Série I* **292**, 146–151.

Mira, C. [1987] *Chaotic Dynamics: From the One-Dimensional Endomorphism to the Two-Dimensional Diffeomorphism* (World Scientific, Singapore).

Mira, C., Fournier-Prunaret, D., Gardini, L., Kawakami, H. and Cathala, J. C. [1994] "Basin bifurcations of two-dimensional noninvertible maps: Fractalization of basins," *Int. J. Bifurcation and Chaos* **4**(2), 343–381.

Mira, C., Gardini L., Barugola, A. & Cathala J. C. [1996] *Chaotic Dynamics in Two-Dimensional Noninvertible Maps* (World Scientific, Singapore).

Mira C. [1996] "Some properties of two-dimensional (Z_0-Z_2) maps not defined in the whole plane," *Proc. ECIT96 Urbino, Italy, Sept. 96, European Conf. Iteration Theory*, in "Grazer Mathematische Berichte", to appear.